550 | März 1995

SCHRIFTENREIHE SCHIFFBAU

Uwe Gietz und Jürgen Kux

Flow Investigations on the Hamburg Testcase Model in the Wind Tunnel

TUHH
Technische Universität Hamburg-Harburg

Flow Investigations on the Hamburg Testcase Model in the Wind Tunnel

Uwe Gietz, Jürgen Kux Hamburg, Technische Universität Hamburg-Harburg, 1995

ISBN: 3-89220-550-7

Schriftenreihe Schiffbau
Schwarzenbergstraße 95c
D-21073 Hamburg

http://www.tuhh.de/vss

INSTITUT FÜR SCHIFFBAU DER UNIVERSITÄT HAMBURG

Bericht Nr. 550

Flow Investigations on the Hamburg Testcase Model in the Wind Tunnel

Uwe Gietz
Jürgen Kux

März 1995

Abstract

Investigations of the so called "Hamburg Test Case", the wind tunnel model of a real built ship (Container Carrier "Ville de Mercure") were performed.
The flow around one quarter of the the model was measured in the wind-tunnel with a three-component Laser-Doppler-Velocimeter. The measurements were taken in transverse planes. One measuring plane was located at the main frame, five at the stern and another one in the far wake. The area covered by the grid of measuring points in each station extends outwards at least to the extent of the main frame, except at the main frame station. The extent of the inner part is limited by the contour of the frame at the given X-station and by the symmetry plane of the flow. The evaluation of the measurements results in the presentation of the vector field of mean velocity and one component of the Reynolds-Stress-Tensor.

Additionally the wall pressure at the stern is determined by pressure tabs on the hull. A visualization of the directional field of the wall shear stress distribution was performed in the same section. The pattern of the flow near to the plane of the propeller was visualised by a laser light sheet.

Zusammenfassung

Das Untersuchungsobjekt ist der "Hamburg Test Case", das Windkanalmodell einer realen Schiffsform (Containerschiff "Ville de Mercure").
Das Strömungsfeld in einem Quadranten des Modells wurde im Windkanal mit einem Dreikomponenten Laser-Doppler-Velocimeter bestimmt. Die Messungen erfolgten in mehreren Spantebenen. Eine Messebene liegt am Hauptspant, fünf im Heckbereich und eine weitere im fernen Nachstrom. Die Ausdehnung der Messpunktraster überdeckt etwa die Abmessungen des Hauptspants mit Ausnahme am Ort des Hauptspants selbst. Die Begrenzung nach innen wird durch die jeweilige Spantkontur vorgegeben bzw. durch die Symmetrieebene der Strömung. Die Auswertung der Messungen erlaubt die Darstellung des Vektorfeldes der mittleren Geschwindigkeit und einer Komponente des Reynoldstensors.

Zusätzlich wurden im Hinterschiffsbereich Messungen des Wanddrucks durch Anbohrungen am Modell durchgeführt. Ein Anstrichversuch machte das dortige Richtungsfeld der Wandschubspannungen sichtbar. Eine Sichtbarmachung des Strömungsfeldes kurz vor der Propellerebene wurde durch einen Laserlichtschnitt erreicht.

1 Introduction

Experimental investigations on ship models have long since been the basis for the prediction of the full-scale design characteristics. The different components relevant to the flow, the fluid, hull, rudder, propeller and free surface, which are interactive in reality, bring about such a high complexity of the entire process that, even in model investigations, not all aspects can be considered at the same time in the same accuracy. Depending on the extent and on the type of the experiments it is possible to get informations about integral characteristics of the flow as well as detailed information about the velocity and pressure field around the model. Due to the large difference of the Reynoldsnumber between the model scale and the full scale of the ship, the predictions of such characteristics for the real ship partly fail to give the correct values.

Another approach for predicting the flow characteristics is the attempt by computational fluid dynamics (CFD). It is successful in aeronautical applications where the approximation of only weak coupled flow domains with two-dimensional flow is allowed. In this case, several well-known (and helpful) empirical laws and approximations concerning the development of two-dimensional flows can be applied. In naval hydrodynamics the flow is mainly three-dimensional. Thus we have to leave the domain of validated use of the mentioned approximations. Furthermore, the step from two to three dimensions implies much more than only an increase of the involved volume. The interaction between different parts of the flow becomes much more complicated. Analytical solutions, hard to find even for two-dimensional flow, exist only for a few exceptional cases. The only way to solve the hydrodynamic equations in the three-dimensional case is by numerical procedures, leading to large systems of coupled equations. The numerical procedures becomes even more complicated when the flow is turbulent. The often used Reynolds-Averaged-Navier-Stokes-Equation (RANSE) reduces the complexity of the problem by time-averaging, so that solutions of the hydrodynamic problems can be obtained without using super-computers. But this simplification, i.e. solving only equations of time averaged values, leads to another difficulty. A substitution of velocities by their mean value and their variance introduces some unknown relations between the mean flow and the variance elements (e.g. the Reynolds-Stress-Tensor). Due to a lack of knowledge of three-dimensional flow, these relations often are approximated as in the two-dimensional case. Therefore we are left with an uncertainty in the computed results, particularly in the areas where the flow is three-dimensional.

The only way to get reliable informations of such flow are experimental investigations. At the "Institut für Schiffbau" (IfS), such investigations have systematically been carried out on a number of ship models in the wind tunnel. First by using pressure probes and later by the use of Laser-Doppler-Velocimetry (LDV), the signals being processed by a correlator type device. Now we use a three-component LDV-System, which was employed to investigate the flow of the windtunnel models HSVA-tanker and HSVA2-tanker. It was thus possible to obtain data sets giving detailed information on the mean velocity and turbulence distribution of the flow. They are well-suited to be used as test cases for CFD methods [1] [4] [11].

The actual measurements reported here extend these former investigations of other models by measurements carried out on on new case of entirely different quality, the so called "Hamburg Test Case" (HTC). The experimental investigations were part of broad research activities of the "Bundesministerium für Forschung und Technologie" (BMFT). The areas of investigation of the different reasearch groups were coordinated. Thus the influence of many factors on the flow as scale, free surface, current fluid, model with/without propeller can be judged.

Various types of investigations have been carried out, they cover a broad range of methods and were carried out at different scales of the model. Data-sets from the full-scale ship, from a towing tank model and a wind tunnel model are now available. The main part of the investigations is finished and its results are documented in computer readable sets of data. Therefore they offer a versatile reference for the validation of results of CFD methods.

These data comprise:

- Full Scale Ship
  Scale 1:1, Lpp = 153.7m
  Measurement of the axial component of the mean velocity field at station 5.26 m upstream of the aft perpendicular (1.3 m before the propeller plane)

- Towing Tank Model
  Scale 1:24, Lpp = 6.4m
  Measurements of resistance and propulsion at different Froudenumber
  Measurements of the wave pattern
  Wallpressure measurements on the hull
  LDV-measurements of mean velocity field in several transverse planes in the stern region

- Wind Tunnel Model
  Scale 1:57, Lpp = 2.7m
  Wall pressure measurements on the hull
  Pressure measurements in the flow field around the hull
  Visualiziation of flow pattern
  Visualiziation of wall shear stress directional field
  LDV-measurements of mean velocity field and turbulence characteristics in several transverse planes at the bow, at the main frame, in the stern region and in the far wake

2 Test Case

As test cases for validation of CFD results for the flow around ship models in the past, in the 1990 workshop in Gothenburg [17] and in the 1994 workshop in Tokyo [10] the so called HSVA1-tanker and the HSVA2-tanker (the so called "mystery case") were chosen. Both hulls have been particularly difficult examples for the algorithms of CFD, but as full scale ships they were never built. The actual case described in this report is the flow around a container carrier with bulbous bow, a slender midship and an approximately non-separating flow at the stern and is thus a model of a realistic hull form (fig. 1). The length, beam, draught[1] blockcoefficient and scale are given below.

Lpp	=	153.7	m
B	=	27.5	m
Tcwl	=	10.55	m
Tfp [1]	=	9.2	m
Tap [1]	=	10.3	m
Cb	=	0.645	
Scale	=	1:57	

Table 1 Main Particulars of "Hamburg Test Case"

The wind tunnel model, a so called "double model", consists of two identical halfs. The plane through the undisturbed waterline serves as a mirror-plane, as symmetry-plane to the model. The conditions of trim (0.41^o) and sinkage were chosen so that the full-scale measurement conditions were reproduced in the wind tunnel model, which leads to a slight decrease of draught toward the bow. The model is manufactured without rudder, propeller or any other appendages. This corresponds with the conditions and restrictions used in most CFD procedures.

The incident velocity is chosen as $U_\infty = 27$ m/sec. With the length Lpp of the model this gives a Reynolds Number of $5 \cdot 10^6$. The transition to turbulent flow in the boundary layer is effected by a vertical roughness strip. Its X-location ist just behind the bulbous bow at the intersection of the "waterline" and the stem of the model.

Differences between the CFD-grid representing the hull and the real form of the model would hinder the comparison between numerical results and experiments. In order to optimize the correspondence of the numerical and the models hull, its body plan was digitized. The digitized data were converted into a high-density net of the hull geometry, serving as data set for numerical calculations as well as data set for manufacturing the model with a computer controlled five-axis milling machine.

The model is suspended in a measuring cage, the "Slotted Wall", with a length of 5 m and a diameter of 1.2 m (fig. 2). It is supported by 8 wires (Ø 1.4mm) at stations 0.15 Lpp and 0.76 Lpp downstream of the forward perpendicular. One pair of wires is installed at each of four points of the hull which are located in the symmetry plane of the model.

By the use of the Slotted Wall the flow along the full length of the measuring section is hindered to decay at the border to the surrounding air at rest, as it would rapidly do otherwise. Due to the construction of the measuring cage an equalization of the static pressure takes place, leading to pressure conditions eqivalent to those in an unlimited flow.

[1] Measurement conditions: Tfp, Tap, draught of the prolonged bottom of the ship at the forward and at the aft perpendicular

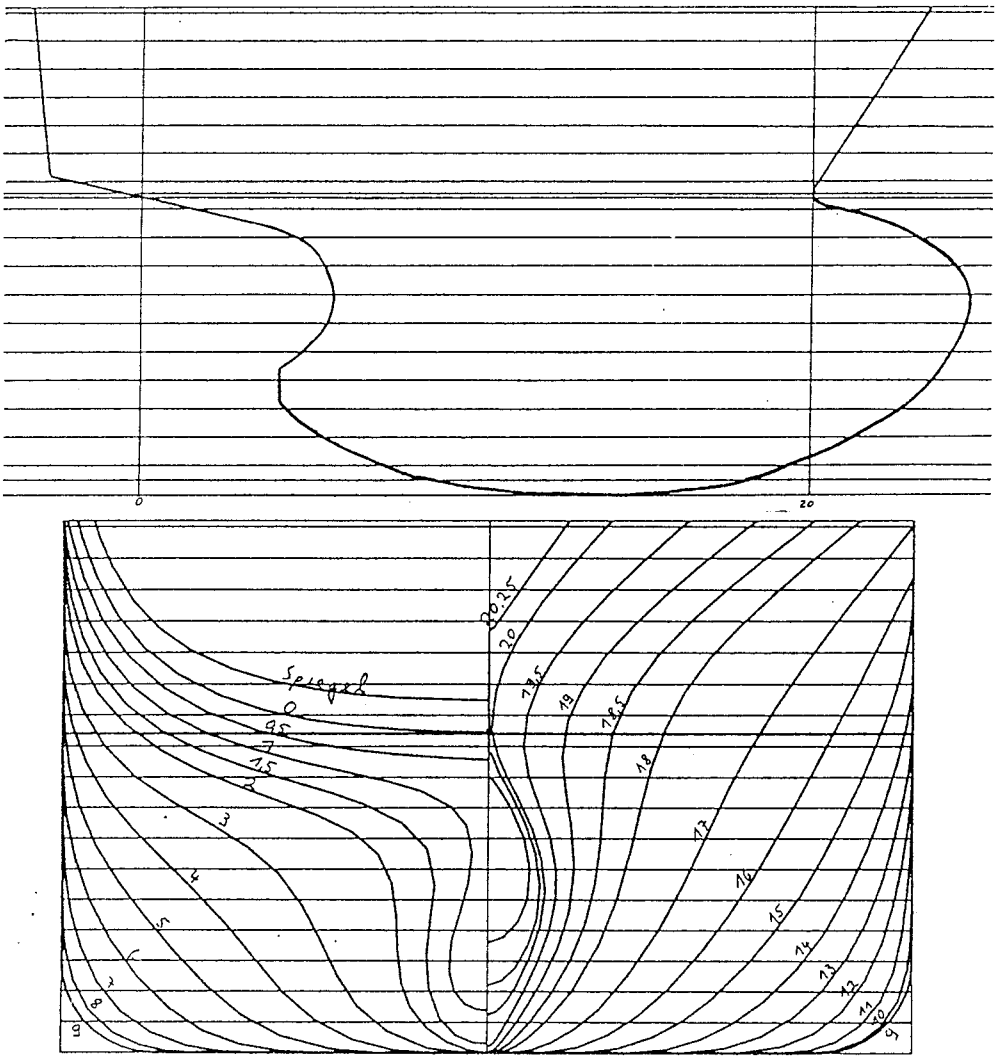

Fig. 1 Body plan of the "Hamburg Test Case"

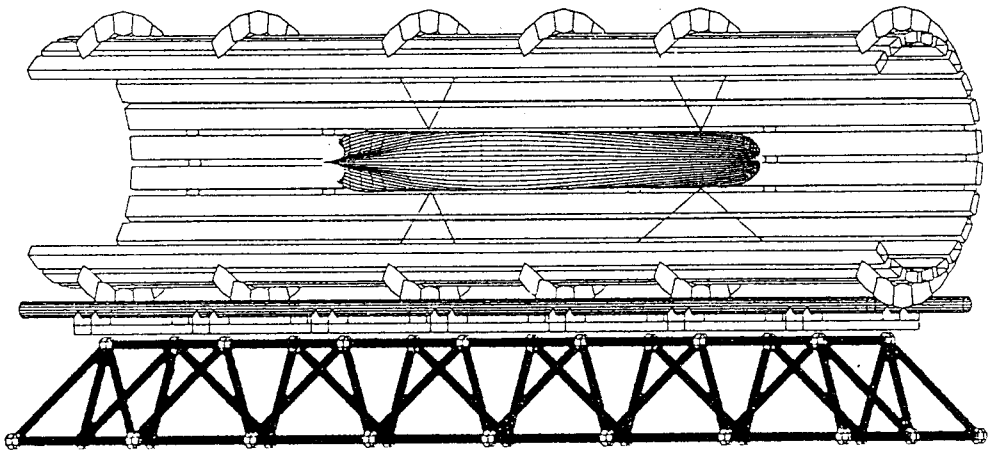

Fig. 2 Wind Tunnel Model and "Slotted Wall"

3 Setup

The quality of the data is based on a wide range of single factors. A good integration of equipment and the accompanying hardware and software is needed to ensure extensive and detailed measurements.

3.1 The Wind Tunnel

The wind tunnel of the IfS is of the so called "Göttinger type". Two modes of operation are available, either with closed circuit flow (mostly used in this mode) or with open outlet behind the impeller and inlet in front of the setting-chamber.
The low level of turbulence is obtained by a huge setting chamber with built-in duster and rectifier. As a second the large contraction ratio of 14:1 is to be mentioned (Setting Chamber 4 x 4 m, Measuring Cage Inside-Ø = 1.2 m).

Technical Data

	Wind Tunnel:	
-	Power	110 KW
-	Max. Velocity	58 or 35 m/sec, depending on diameter of Measuring Section
-	Degree of Turbulence	$< 1\%$
-	Measuring Section	Length 5.5 m, Diameter optional 1.2 or 2.0 m, open Measuring Section
-	Traversing Mechanism	programmable and computer controlled Traversing desk suitable for different measuring setups Basic positioning accuracy 1/100 mm
	Equipment:	
-	Force Detection	6-Component-Balance
-	Pressure Measurements	Stationary transducer with "Hottinger&Baldwin"-amplifier, various types of pressure probes
-	LDV-System	Three component system of "TSI", used in backward scattering off-axis mode, focal length 1200 mm

3.2 Three Component LDV System

The laser velocimeter system consists of one fixed and one mobile part (ref. figure 4). It is thus possible to keep the weight of the actual measuring head (emitting and receiving lens system) below the limiting load capacity of the traversing mechanism.

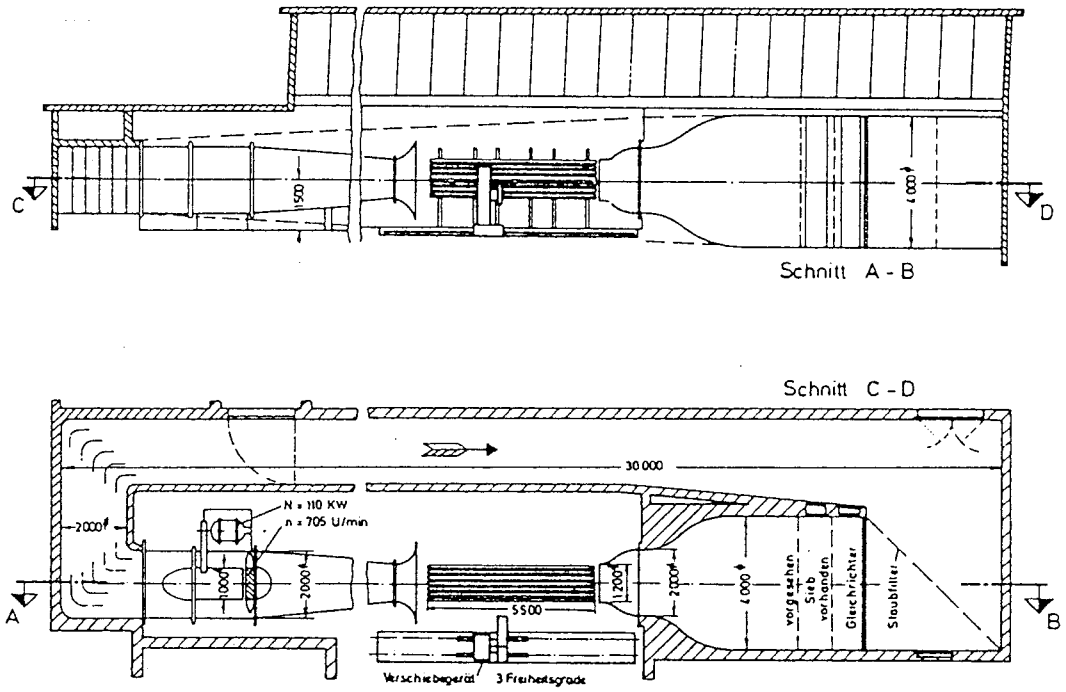

Fig. 3 The Wind Tunnel of the IfS

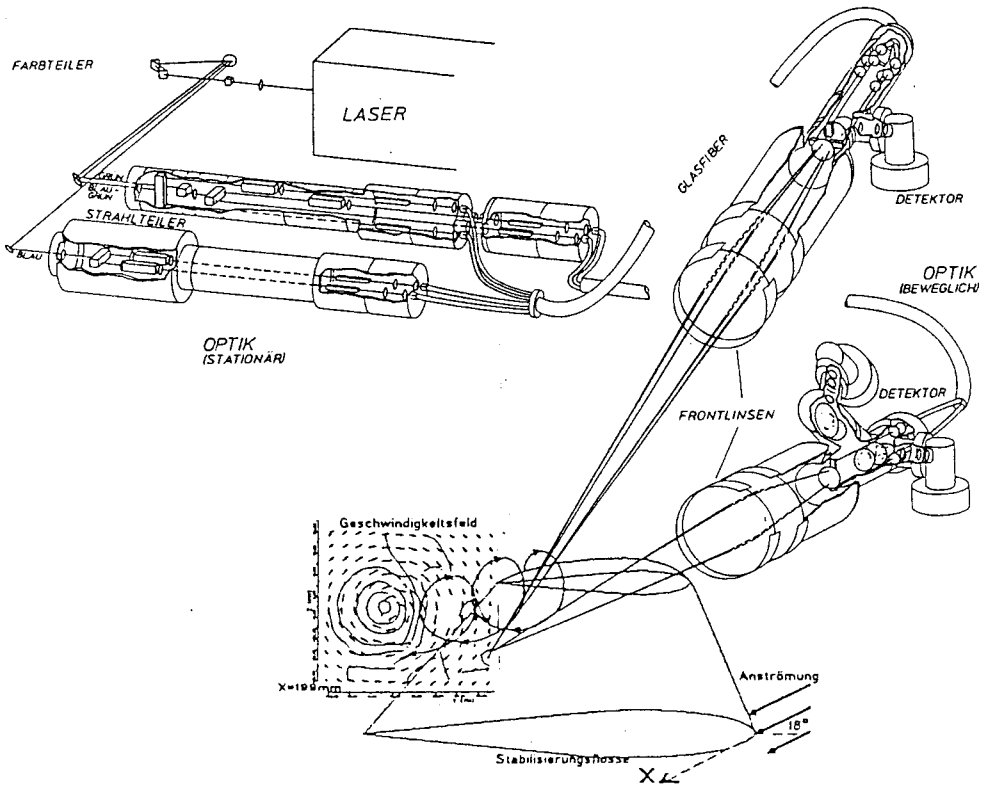

Fig. 4 The Laser Velocimeter System

Stationary Part of the Velocimeter System:

The generation of laser beams, separation of colours, and splitting of the beams are carried out with modules on an optics table. An argon-ion-laser serves as a source for the three colours required in order to measure three components simultaneously (multi line operation). The laser gives a maximum output capacity of 4 W over all lines in TEM00 mode. The polarized laser beam is splitted into its spectrum colours by means of a prism. Employing bragg cells for each single colour makes it possible to determine the sign of the measured velocity component. The wave lengths used for three component operation are

- 514 nm (green, G)
- 488 nm (blue green, BG)
- 476 nm (blue, B)

Mobile Part of the Velocimeter System:

Here the front optics consists of two measuring heads which send and receive along two optical axes which have an inclination of 5^o and 30^o against the horizontal plane. Each beam pair of the measuring heads intersect at a common focus which is the measuring spot, more precisely the measuring volume. Due to the focal length of the optics it is 1200 mm away from the front lenses, much more than the inside radius of the measuring cage. The diameter of the sensitive volume is 0.1 mm ($3.7\ 10^{-5}$ Lpp), its length 0.3 mm ($1.1\ 10^{-4}$ Lpp).

The scattered light from particles crossing this volume is collected by the lens system of the other measuring head, that one, which did not emit. Three photo multipliers serve as detectors for the three colours, each equipped with a pinhole at its input and an interference filter.
The fixed and the mobile part of the LDV-System are connected by glass fibres which conserve the polarization. They transmit the incident laserlight of the three different colours through six single fibres with a nominal efficiency of 50 %.

4 Methods

The use of different experimental methods leads to global and qualitative information as well as to local and quantitative results. The different kinds of methods complement each other. Results from "time saving" experiments were used to optimize subsequent time intensive measuring methods.

4.1 Visualisation of Flow

The structures in the stern flow can be visualized by means of a laser light sheet. A laser beam is fanned out through a cylinder lens into a light sheet. This sheet is positioned transversally near to the propeller plane.

For visualisation purposes, the model flow is probed by smoke, a kind of oil mist, introduced at approximately 600 mm (0.2 Lpp) upstream of the plane of the propeller. Structures of the complex velocity field of the flow, normally only roughly visible, are clearly visiualized in the area of the laser light sheet, the structures reduced to a two-dimensional pattern. By this visiualization it was possible to identify features of the flow which were previously hidden. They are documented on a video tape.

4.2 Visualisation of Wall Shear Stress

The physical processes in the flow taking place close to the wall determine the field of the wall shear stresses, which are, due to technical reasons, difficult to measure. An insight into the directional field of the shear stresses can be gained by coating the model with paint.

The hull surface in the stern area of the model was coated on its upper and lower half, then the wind tunnel started. The liquid material on the surface is now moved by the flow adjacent to the model into the direction of the local acting forces. Thus the resulting pattern reflects thereby the directional orientation of the local acting forces. In areas of converging streamlines, this movement is clearly visible as "surface flow" which induces a transportation of superfluous liquid material.

The experiment is documented on a video tape and on pictures taken at its final stage.

4.3 Wall Pressure Measurements

The static pressure on the hull of the model is determined by both, the local flow immediately near the surface (vortices, separation) and the global structure of the flow. For an investigation of the pressure distribution without an additional disturbance, pressure tabs on the hull are used. The hull had been equipped with 45 holes (inside-Ø 0.8 mm) at six different stations, at a distance of about 130 mm (0.05 Lpp) from each other.

Each pressure tab is successively attached to a transducer which is located outside the measuring cage. Its pressure was measured and simultaneously the pressure PV of the setting-chamber of the wind tunnel. Each measured pressure is normalized with the corresponding PV.

The accuracy of the results of the pressure measurements depends on the quality of the transducer combined with its electric amplifier and the device to digitize the analog signal quantity. A further error source could be an unsufficient mechanical smoothness of the surface close to the pressure tab. If in its surrounding there is a furrow or an edge, it is most likely to get considerable differences between the measured and the real pressure value. The pressure data show that these effects seems to be neglible in this case.

4.4 Laser-Velocimetry

An LDV-System makes it possible to measure the local instantenous velocity without disturbing the flow, by means of intersecting beams of laserlight [6] [7]. The measurement principle is based on the Doppler-Effect. Incident laser light is scattered by particles (Seeding) in the flow. The frequency of the scattered light is shifted by a small amount Δf proportional to the velocity of the particle. A simplification of the method can be obtained by use of the "crossed-beam-technique" which is applied here. The relationship between the velocity of the particle and the shift in frequency is given by

$$\Delta f = \frac{1}{\lambda} \frac{\vec{v} \cdot (\vec{s} - \vec{l})}{1 - \frac{\vec{v} \cdot \vec{s}}{c}}$$

Δf frequency shift of the scattered light
λ wavelength of the laserlight
$\vec{v}$ velocity of the scattering particle
$\vec{l}$ direction of incident light
$\vec{s}$ direction of scattered light to detector

The LDV-System which is used here is capable to measure all three components of the instantenous velocity vector. For that purpose three pairs of laserlightbeams of different colour are used. The three photomultipliers single out the information of one velocity component by use of narrowband interference filters. These only allow the light from one pair of laserbeams of determined colour (that means one velocity component) to get through to the corresponding detector. All three pairs of laser light beams intersect at one common location which serves as the sensitive volume of the LDV-System.

The evaluation of the signal of a single particle is performed by counters. They are used to transform the electric signal from a photomultiplier into a single digital value for its frequency (i.e. corresponding to a velocity component). With a built-in zero-crossing counting method the frequency of the signal is calculated. The accuracy of a single detected frequency is limited by two factors. On the one hand, the higher the accepted limiting percentage of deviation of frequency inside a single signal, the worse the signal-to-noise ratio of the data. On the other hand, the lower the limiting percentage, the lower the rate of validated data. We used an accuracy of 1 %, the lowest percentage limit of the counters. Thus a large amount of nearly "valid" signals was singled out. To ensure reliable data, we accepted only the signals with "high" signal-to-noise ratio.

The mean velocity at each point is obtained as the average over a data set of 300 single measurements of the instantanous velocity. A gaussian probability density function is fitted to the histogramme representing the probability distribution of the data set of one velocity component. The mean and width of the fitted function give the required values of the mean velocity and turbulence intensity respectivly. The accuracy of the calculated mean value is, therefore, much better than the mentioned accuracy of a single measurement. Measurements of the flow in the open test-section of the wind tunnel validated the theoretical accuracy-limit of the mean to an order of less then 0.1 %.

In order to get data from different locations, the sensitive volume is displaced by traversing the optical system of the laser velocimeter. Typically, the distance between two measuring points is only a few millimeters, much more than the accuracy of the traversing system of 0.01 mm. Thus, every location can be entered and it is possible to reproduce precisely its coordinates.

5 Results

In the figures of the results, the coordinate system of the LDV-measurements is applied (ref. Appendix, fig. 34). Additionally the X-coordinates of the measured planes are given in units of Lpp, the origin located at the forward perpendicular.
The transformation from the LDV-coordinate system to the non-dimensionalized Lpp-coordinate system (the coordinates normalized with Lpp) is given by

$$X_{Lpp} = X_{LDV}/Lpp + 0.95550$$

$$Y_{Lpp} = Y_{LDV}/Lpp$$

$$Z_{Lpp} = Z_{LDV}/Lpp$$

$$Lpp = 2696.5 \text{ mm} \qquad \text{corresponding to the wind tunnel model, scale 1:57}$$

The check stations of the various types of experiments and their relative positions are shown below:

Flow Pattern

X mm	50
X/Lpp	0.9

Shear Stress Pattern

X mm	-400	30
X/Lpp	0.81	0.96

Wall Pressure

X mm	-638	-385	-259	-133	-27	8
X/Lpp	0.719	0.813	0.859	0.906	0.945	0.959

LDV-Measurements

X mm	-1093.4	-50.0	-29.0	-8.0	9.0	30.0	900.0
X/Lpp	0.55001	0.93696	0.94474	0.95253	0.95884	0.96662	1.28926

The results are presented in two ways:

i) The distribution of the measured data along the girth at a given station will be shown

ii) The spatial structure of the measured data in a plane is represented by arrows or by lines of constant value. They represent the content of varying data such as pressure coefficient, axial velocity, transverse velocity and one component of the Reynolds-Stress-Tensor.

The values of the measured pressure data are normalized with the stagnation pressure, velocities with the incident velocity U_∞ and the component of the Reynolds-Stress-Tensor with U_∞^2. The labeling of the isolines at different stations is given below:

Isoline labels of Cp, all stations:

-0.12 -0.09 -0.06 -0.03 -0- 0.03 0.06 0.09 0.12 0.15 0.18 0.20

Isoline labels of u, Main Frame:

0.50 0.60 0.70 0.80 0.90 1.00 1.01 1.015 1.02

Isoline labels of u, Propeller Boss:

0.10 0.20 0.30 0.40 0.50 0.60 0.70 0.80 0.90 0.94 1.00

Isoline labels of u, Far Wake:

0.78 0.80 0.82 0.84 0.86 0.88 0.90 0.92 0.94 0.96 0.98 0.995

Isoline labels of u'^2, all stations:

.002 .004 .006 .008 .010 .012 .014 .016

5.1 Flow Pattern

The smoke probe was positioned at several places to evaluate the different upstream areas of interest whose stream lines fall into a certain domain at the stern. It became clear that there exist neighbouring flow-areas at the stern where fluid provenient from non-neighbouring upstream areas concentrates.

The visiualized vortex structures should be put in forward too. The video documentation shows clearly the bilge vortex, its rotation transports fluid material from outside upwards and inwards towards the ship hull. In the area near to the surface there is a "highspeed" flow directed downward. This behaviour is found from the waterline almost down to the keel. At the keel a second vortex is existent, but its visible extent seems to be restricted to an area very close (5 to 10 mm) to the surface.

5.2 Wall Shear Stress Pattern

The evaluation of the experiment is based on photos which give the information about the final stage of the visiualisation, when the paint has become dry. Further on we evaluated the video documentation too, which provided us with information about the dynamic development of the resulting structures.

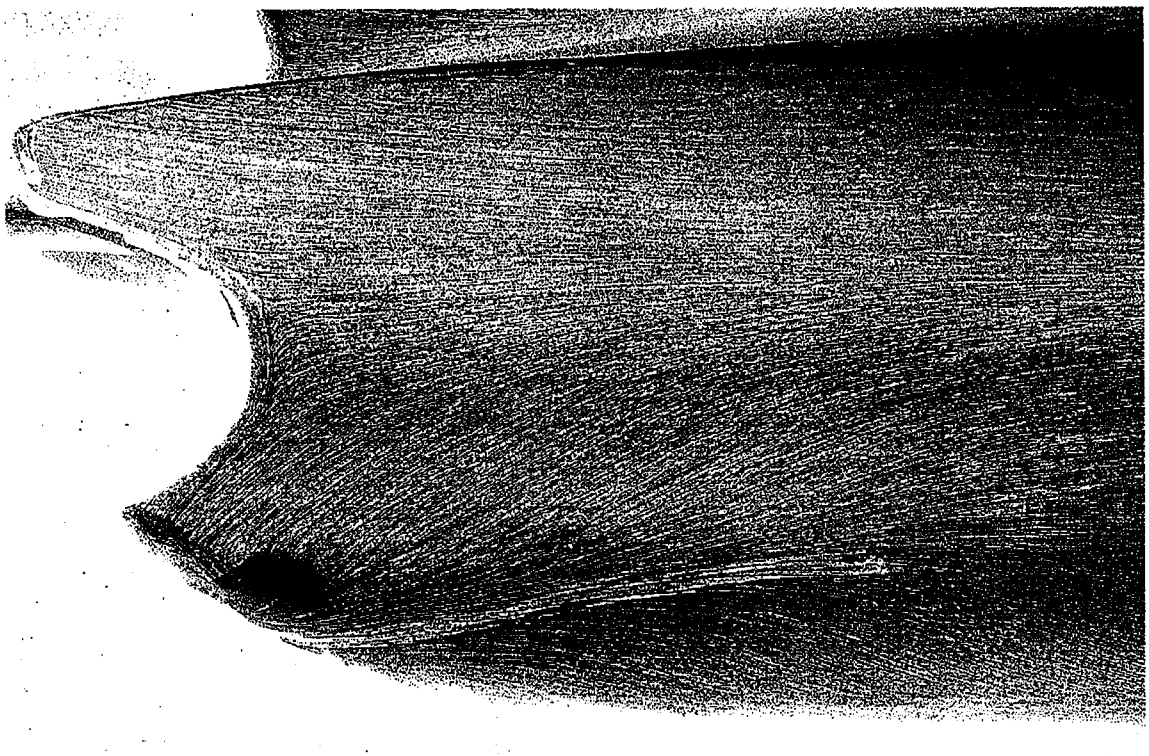

Fig. 5 Visiualisation of shear stress directions

The pattern of the shear stress visiualisation gives an immediate impression of the directional field of the shear stress (limiting streamlines) at the surface. The approximate rectilinear limiting streamlines in the upstream region visibly change their directional behavior approaching the stern.
We can distinguish that area of the surface which feeds the upward flow into the upper rear part from that one delivering the fluid which is turned downwards to the propeller boss. A third flow section from under the hull comes upward and converges with the mentioned downward directed flow. We may call the area of convergence one of line separation since the incompressible fluid there has to deviate outward, away from the hull surface. Finally at the stern there is a bifurcation point.

A clear indication of separation can be seen at the contour of the stern. We see an area of flow separation (width: only a few millimeters upstream). It is marked with a characteristic change in the shear stress pattern. The border of this area is clearly visible by a thin "stop line". The flow immediately above the surface is obviously pushed aside (on the surface) when reaching this line. This behavior is best visible from the video documentation.
A very characteristic feature is the parallel course of the "stop line" and the contourline of the propeller boss. Even the almost rectangular bend of the contourline is reproduced by the "stop line".

5.3 Wall Pressure

The figures 6 to 11 show the coefficient of wall pressure Cp as a function of the girth-length, scaled 0 to 1 from the keel to the waterline. The only exceptional case gives X = 8.36 (fig. 11) where the stern is divided into two parts, one at the waterline and the other at the propeller boss. In this case the measured data and the nondimensionalized girth are related to the upper part of the stern. The pressure measured does not exceed the range of $-0.2 < Cp < 0.3$.

Fig. 6 Cp, girthwise distribution
X = -637.9 mm (0.719)
The pressure coefficient Cp shows only small changes in magnitude over the girth as is to be expected at a location near to the main section. The displacement due to the hull leads to a nearly constant increased velocity with only weak extremes. We find a remarkable deviation from the average value at one point of the keel. This may be caused by the wake of the 0.1m upstream located outlet of the models supporting wires.

Fig. 7 Cp, girthwise distribution
X = -385.34 mm (0.813)
A characteristic feature of the pressure distribution around the girth at this station is a distinct pressure minimum ("low pressure hole") near to the keel. It is embedded in an area of constant low pressure as can be seen from the values measured in the plane at the station upstream of this.

Fig. 8 Cp, girthwise distribution
X = -258.94 mm (0.859)
The course of the pressure distribution is similar to X/Lpp = 0.813 but with more pronounced extreme values. Near to the keel we note the effect of the "low pressure hole".

Fig. 9 Cp, girthwise distribution
X = -132.64 mm (0.906)
Apart from the region in the neighbourhood of the keel all pressure coefficients are positive and increase monotonously towards the waterline.

Fig. 10 Cp, girthwise distribution
X = -27.44 mm (0.9450)
A nearly constant high pressure of Cp = 0.1 governs along the girth. The only exception is a weak pressure minimum located at half of the girth.

Fig. 11 Cp, girthwise distribution
X = 8.36 mm (0.959)
The pressure shows a clear decrease in magnitude approaching the waterline, but all values exceed Cp = +0.15 .

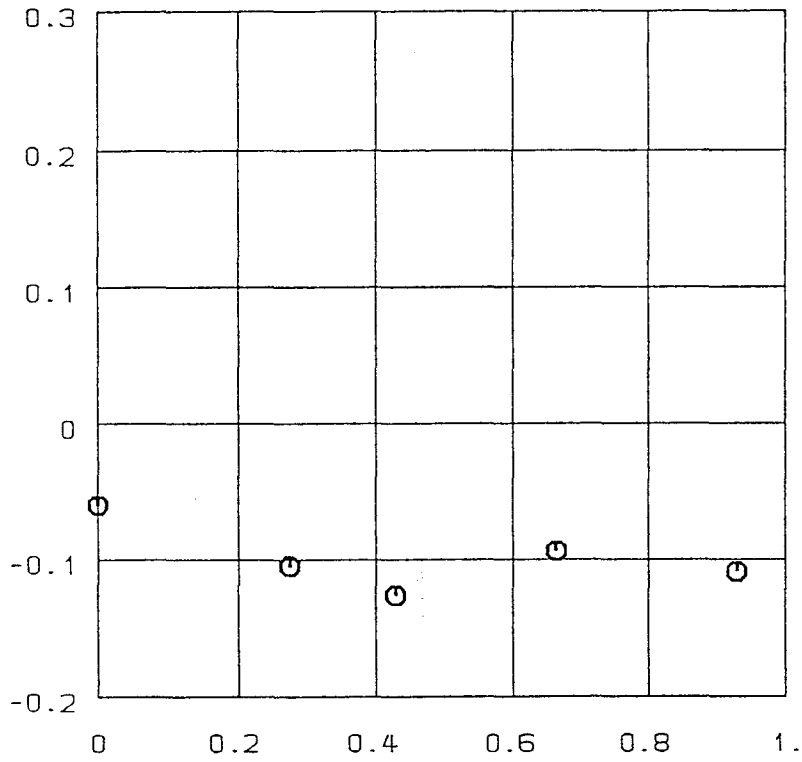

Fig. 6 Cp, girthwise distribution
X = -637.9 mm (0.719)

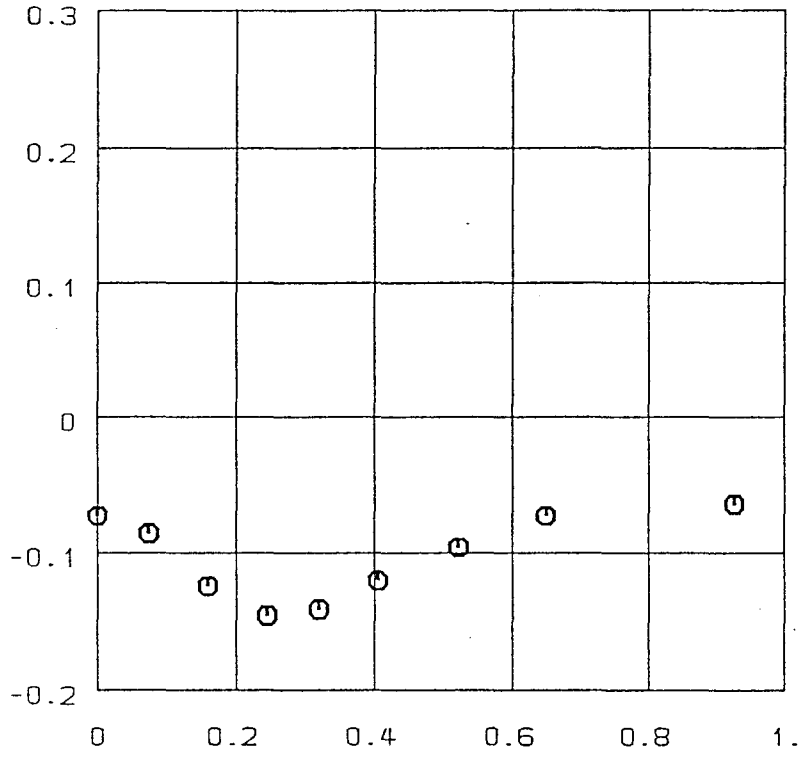

Fig. 7 Cp, girthwise distribution
X = -385.34 mm (0.813)

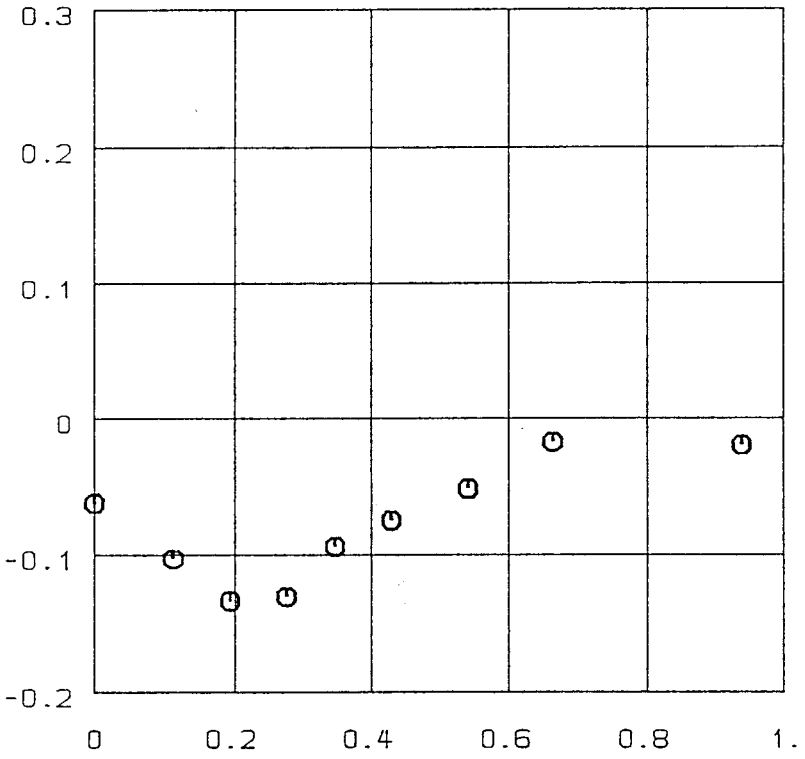

Fig. 8 Cp, girthwise distribution
X = -258.94 mm (0.859)

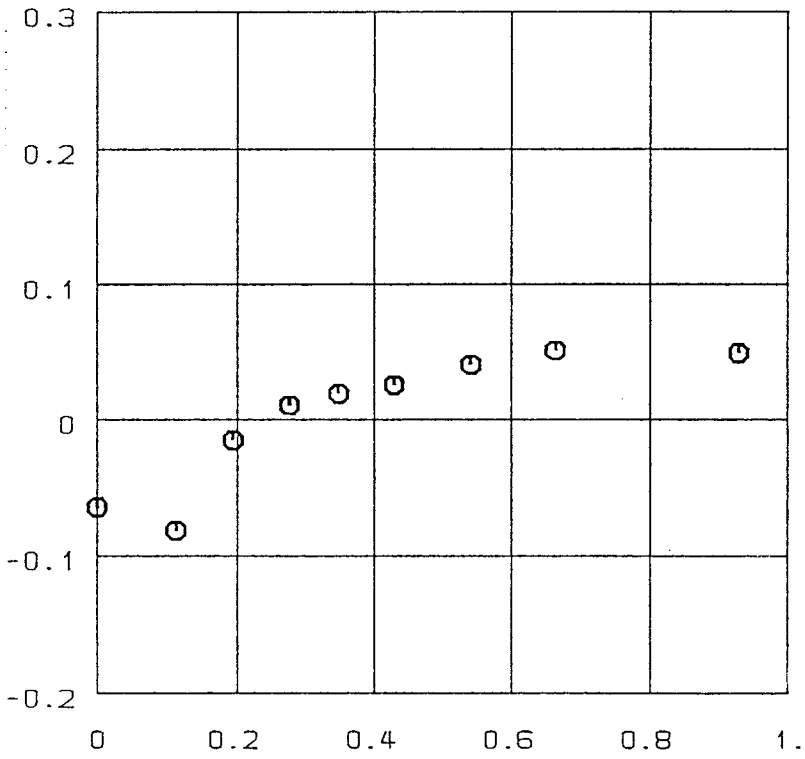

Fig. 9 Cp, girthwise distribution
X = -132.64 mm (0.906)

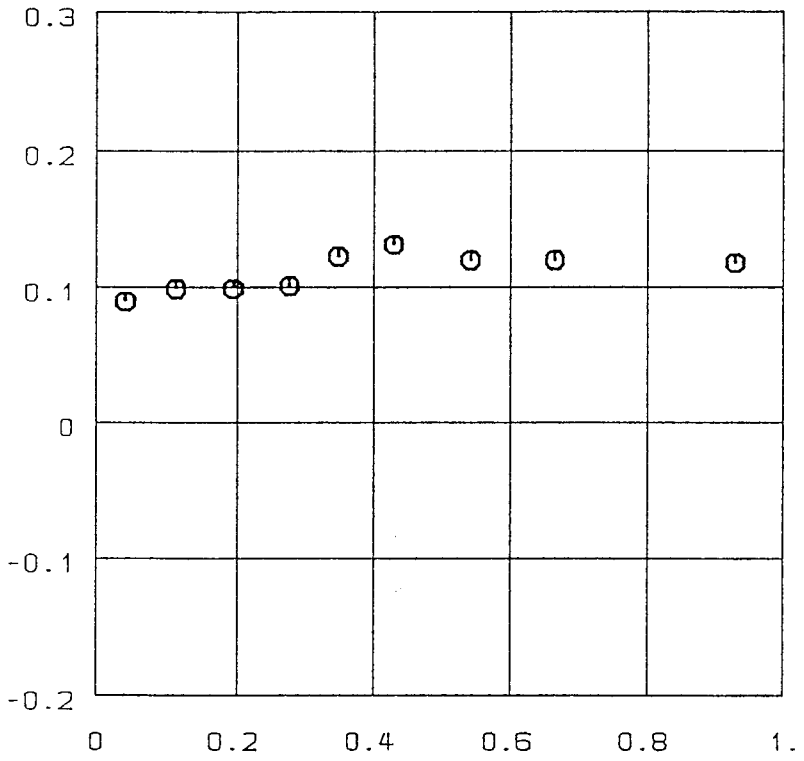

Fig. 10 Cp, girthwise distribution
X = -27.44 mm (0.945)

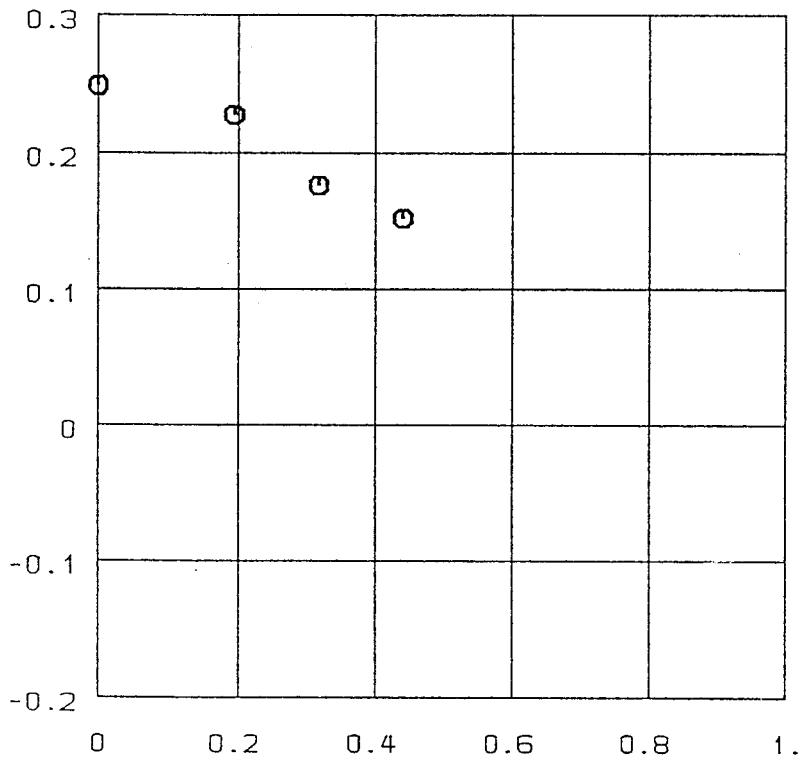

Fig. 11 Cp, girthwise distribution
X = 8.36 mm (0.959)

Figures 12 to 14 represent an overview of the spatial structure of the pressure by means of lines of constant pressure coefficient Cp. An equally scaled figure of each of the three projections in X-, Y- and Z-direction is shown.

Fig. 12 X-Projection of Cp isolines

The pattern of the isolines shows an increase of Cp towards the stern. The spacing between the isolines indicates a mainly homogenous distribution of the increase in X-direction. Solely near to the keel and near to the mentioned pressure minimum we find stronger gradients.

Fig. 13 Y-Projection of Cp isolines

We recognize the homogeneous increase of the pressure in this projection too. The large area occupied by the "low pressure hole" becomes visible.

Fig. 14 Z-Projection of Cp isolines

The view from the bottom makes evident the extent of isolines nearly parallel to the frame. The area is located in that part of the surface of the model (near to the waterline) which forms approximately a slanting plain with unidimensional pressure gradient.
On the other hand we find the area towards the keel with a large curvature of the surface. The isolines become curved too.

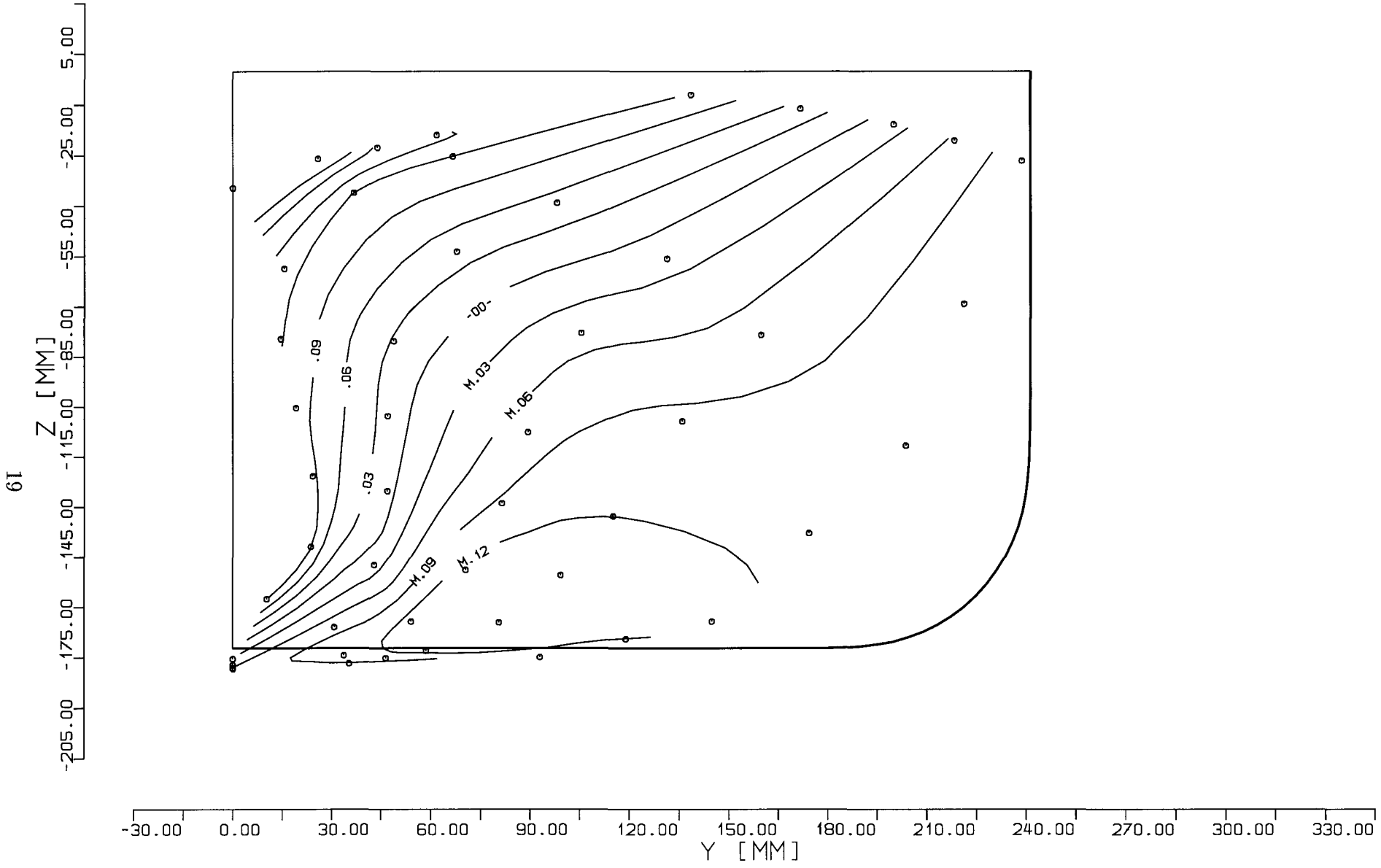

Fig. 12 X-Projection of Cp isolines

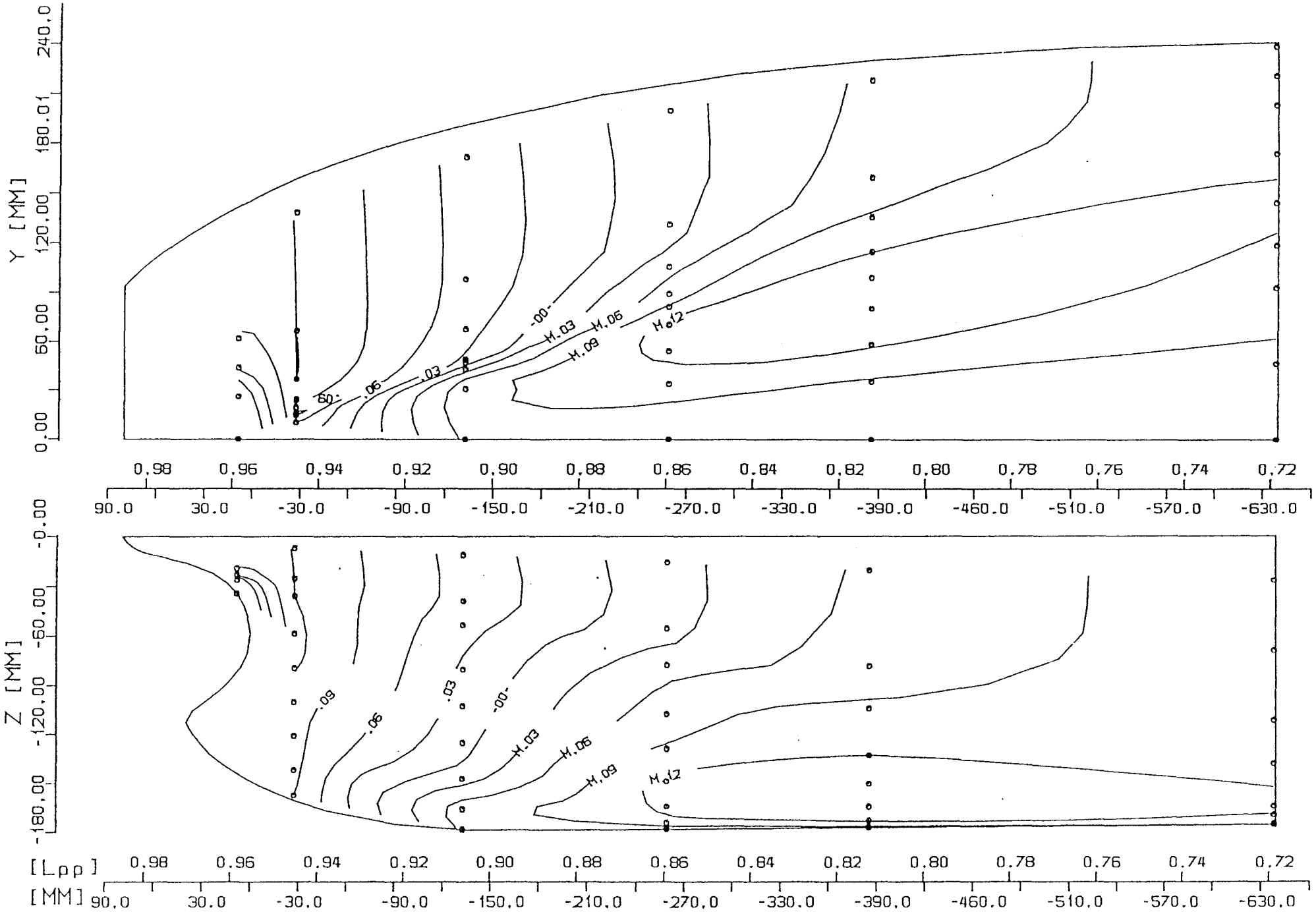

Fig. 13 Y- and Z-Projection of Cp isolines

5.4 LDV-Measurements

The data of the LDV-measurements allow to determine the mean of the local velocity vector and in three directions the fraction of the turbulent energy. The following figures show the distribution of the mean velocity components u, v, w and u'^2, the first component of the Reynolds-Stress-Tensor. Results of more detailed investigations representing the field of elements of the Reynolds-Stress-Tensor will be discussed in a next report.

The LDV-measurements were taken in transversal planes, grouped in three regions:

i) one plane at the main frame

ii) five planes in the region of the propeller boss

iii) one plane shortly downstream of the end of the measuring cage

The area covered by the grid of measuring points in each station extends outwards at least to the extent of the main frame, except at the main frame station itself. The extent of the inner part is limited by the contour of the frame at the given X-station and by the symmetry plane of the flow.

The representation of the axial velocity component is done by isolines of constant component u. The transverse components of velocity v and w are represented by an arrow. The length of the arrow has to be seen in relation to the length of the reference-arrow (U_∞) in the upper right corner of the figure.

In the figures of the flow at the propeller boss the contour of the frame at the respective station is plotted. Additionally the depth of the propeller axis and the depth of the main frame is marked by a tic at the vertical symmetry line. The circle of the propeller is indicated by a dashed line in the figures at stations near the propellerplane. A figure of all frames is supplied in each plot (the scale reduced by a factor 2) as a reference for the change in size of the actual frame (bold line) from an upstream to a downstream station.

Main Frame		Propeller Boss					Far Wake
X mm	-1093.0	-50.0	-29.0	-8.0	9.0	30.0	900.0
X/Lpp	0.55016	0.93696	0.94474	0.95253	0.95884	0.96662	1.28926
Data	u u'^2	u v w u'^2	u v w u'^2	u v w u'^2	u v w u'^2	u v w u'^2	u u'^2

Table 2 Planes of LDV-Measurements

5.4.1 Velocity

i) Main Frame

The isolines of the u-component (fig. 15) show a remarkable reduction of the boundary layer thickness around the bilge. From the waterline along the plain surface towards the bilge we find a constant distance between the isolines and the surface. This changes under the flat surface of the bottom of the ship. The boundary layer thickness increases from its minimum value of 6 mm at the bilge to more than 12 mm at the keel. The seemingly decrease of thickness at the keel may be caused by the plot-software:
Due to mechanical restrictions in traversing the LDV-System there are no measured points in the outer region at the line normal to the keel (z < -190 mm). The increase of velocity up to u = 1.00 is not recorded, therefore lower values of velocity determine the boundary condition of the interpolating grid, on which the isolines are based.

In addition to the large steps of isoline values $\Delta u = 0.1$ the pattern is supplemented by isolines of u = 1.01, 1.015 and 1.02 . It marks the extent, value and region of increased velocity due to the displacement effect of the model. A wide part of the main flow is accelerated to a velocity of up to 1% increase relative to U_∞. The area where this happens reaches from the waterline to the bilge. From here it decreases around the bilge to the level of the incident velocity. In the region under the bottom of the ship we find no distinct overspeed, the maximum of the velocity u = 1.00 is surpassed nowhere.

The isolines u = 1.015 and u = 1.02 indicate an accelerated flow near the bilge. The peak values of 2% overspeed relative to U_∞ lead to a narrow "isle"-isoline from the bilge towards the waterline. Its extent is divided into two parts, which is most likely effected by one or two "erraneous" points between them. Smoothing of the measured data surely would show a closed isoline structure.

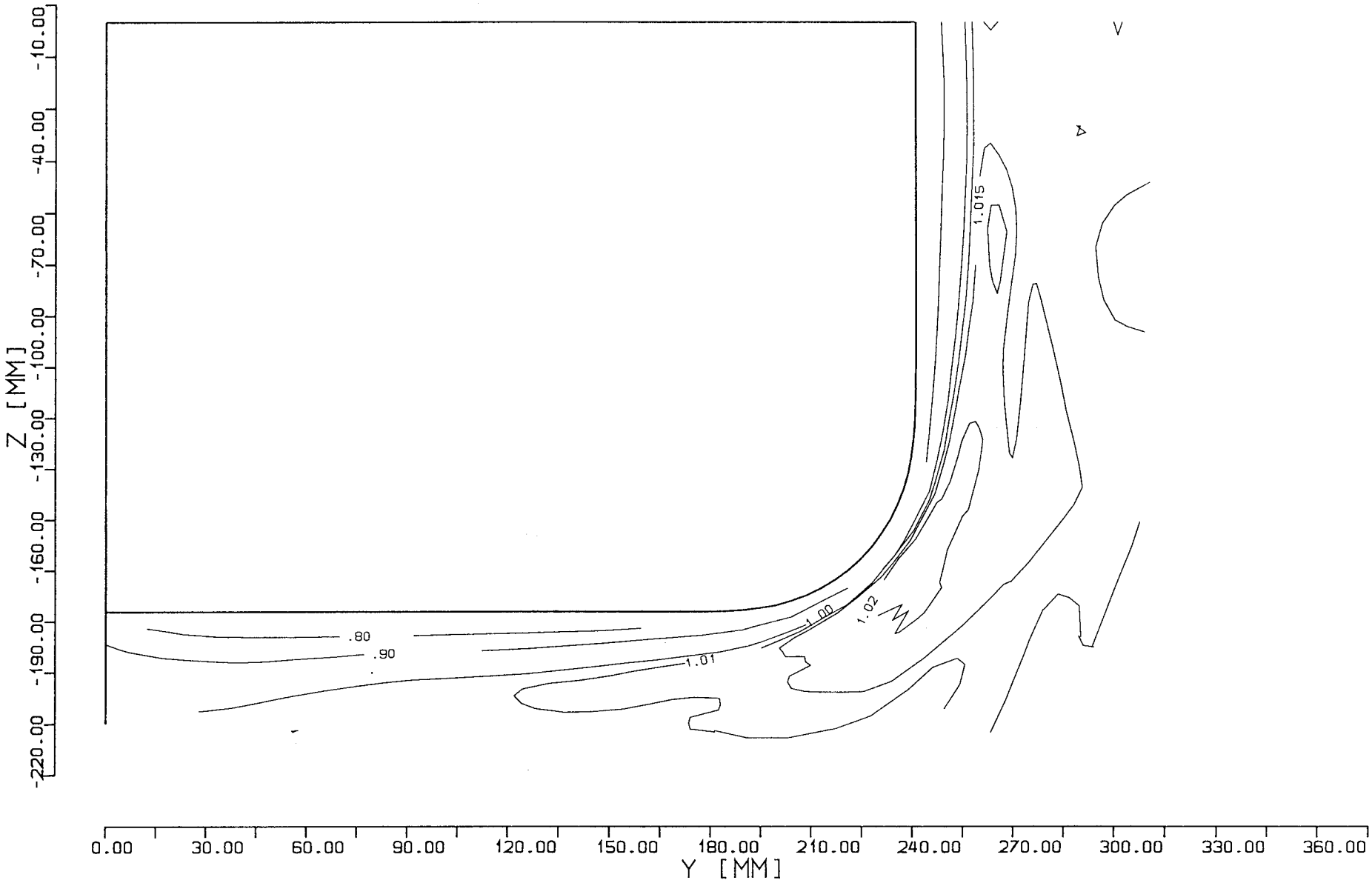

Fig. 14 Isolines of axial velocity u
X = -1093.0 mm (0.55016)

ii) Propeller Boss

The region beneath the propeller boss is very interesting since we can find here a highly threedimensional flow. From the figures of the axial and the transverse components of velocity we get an impression of its structure. The spatial sequence of planes additionally makes clear the different stages in the streamwise development of the flow.

The qualitative behavior of the axial component u in the five planes showes mainly a structure of the same kind (fig. 16 to fig. 20, fig. 26):

A diagonal isoline of u = 0.9 marks the border of the "inner part" of the flow relative to the undisturbed "outer part". An area of strongly decelarated flow (u = 0.3) is visible. This area widens farther downstream as typically registered at other models too (due to its shape this feature has often been titled as "hook" or "pig's ear").

The weak but measurable influence of the diagonally tensed wires (supporting the model in the measuring cage) is clearly reflected by the isolines u = 0.9 and 0.94. The wake of these wires is decelerated a few percent relative to the outer flow. As in former investigations of other models too, the smoothness of the isolines of the wake of the 1.4 mm wires serves as an indication of the high accuracy of the data showing that is possible to examine even structures with only small differences in velocity.

The transverse velocity typically reaches a value of 0.1, but in some cases a maximum value of 0.2 is visible (fig. 21 to 25).
A well-known feature is the upward and inward directed flow in the outer area. Its upward direction is reversed near to the models surface. A downward directed flow of increasing transverse components can be seen ($|w_{max}| = 0.15$).
The development of the bilge vortex over the consecutive X-stations shows an increase of the circumferential components from fig. 21 to fig. 25 .

Some arrows near to the surface (Z = -140 mm) point outwards with a high component "+v". This effect is caused by noise produced through reflected light from the surface. In the oblique coordinate system of the LDV device the second measured transverse component was spoiled by noise signals. By the different sensivity of the measured components against the disturbing light, the other transverse component did not suffer such influence. Therefore the "w" component of the arrow remains undisturbed.
Such points of distorted data are marked by an abrupt change of velocity component to a certain range of magnitude. This makes it possible to recognize these points in the most cases, even if a knowledge of the underlying source of the disturbance is not present.

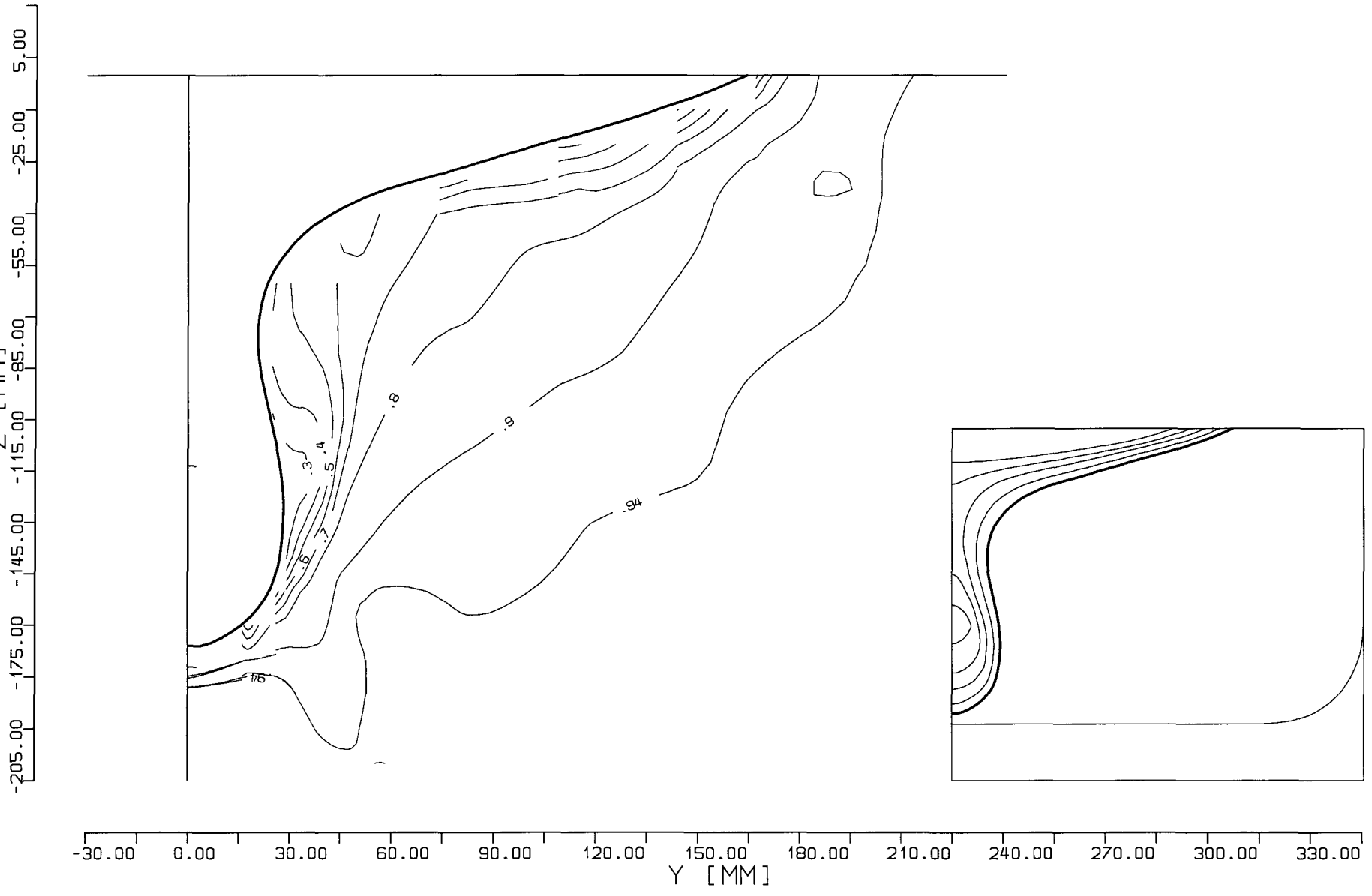

Fig. 15 Isolines of axial velocity u
X = -50.0 mm (0.93696)

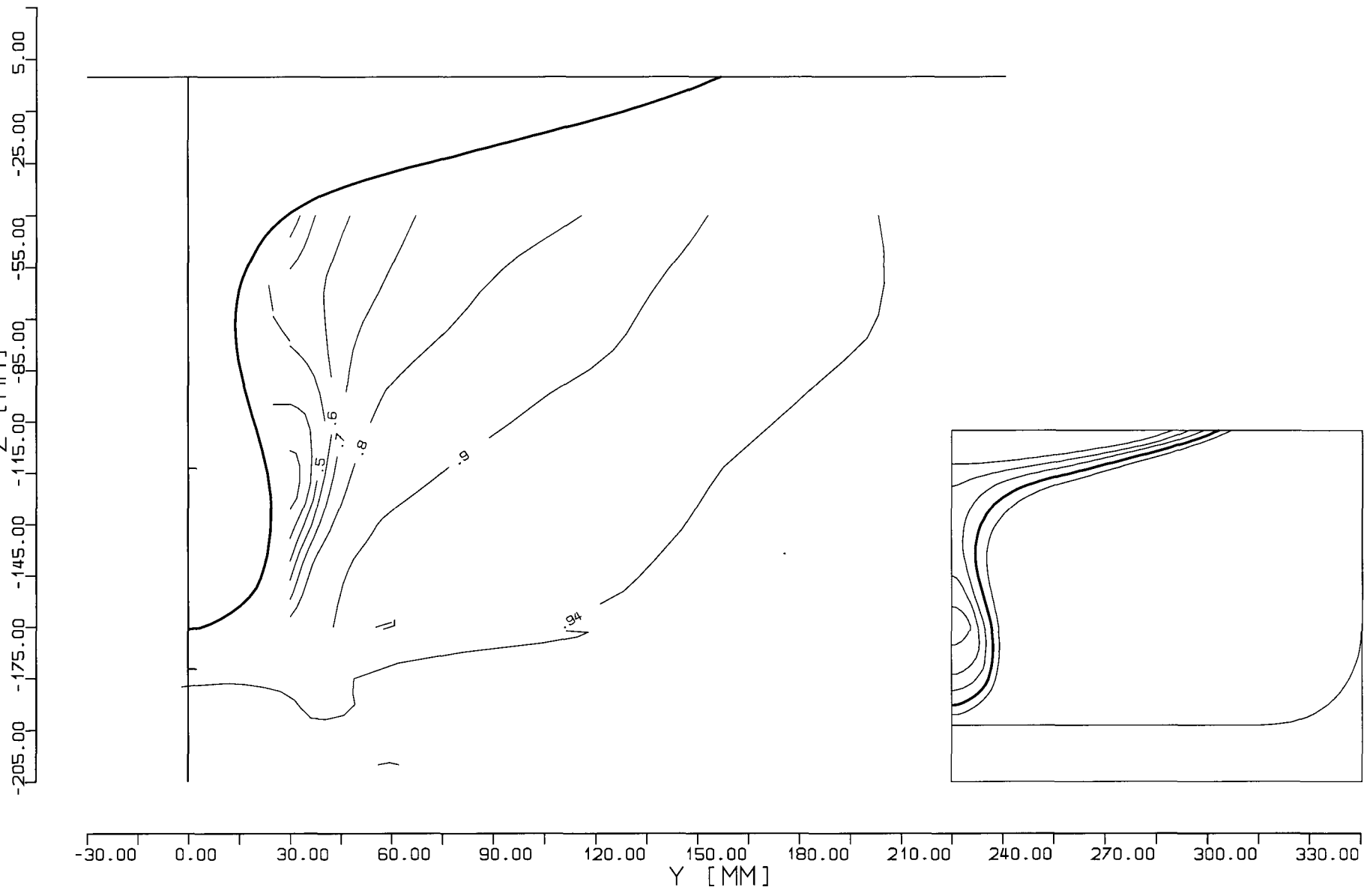

Fig. 16 Isolines of axial velocity u
X = -29.0 mm (0.94474)

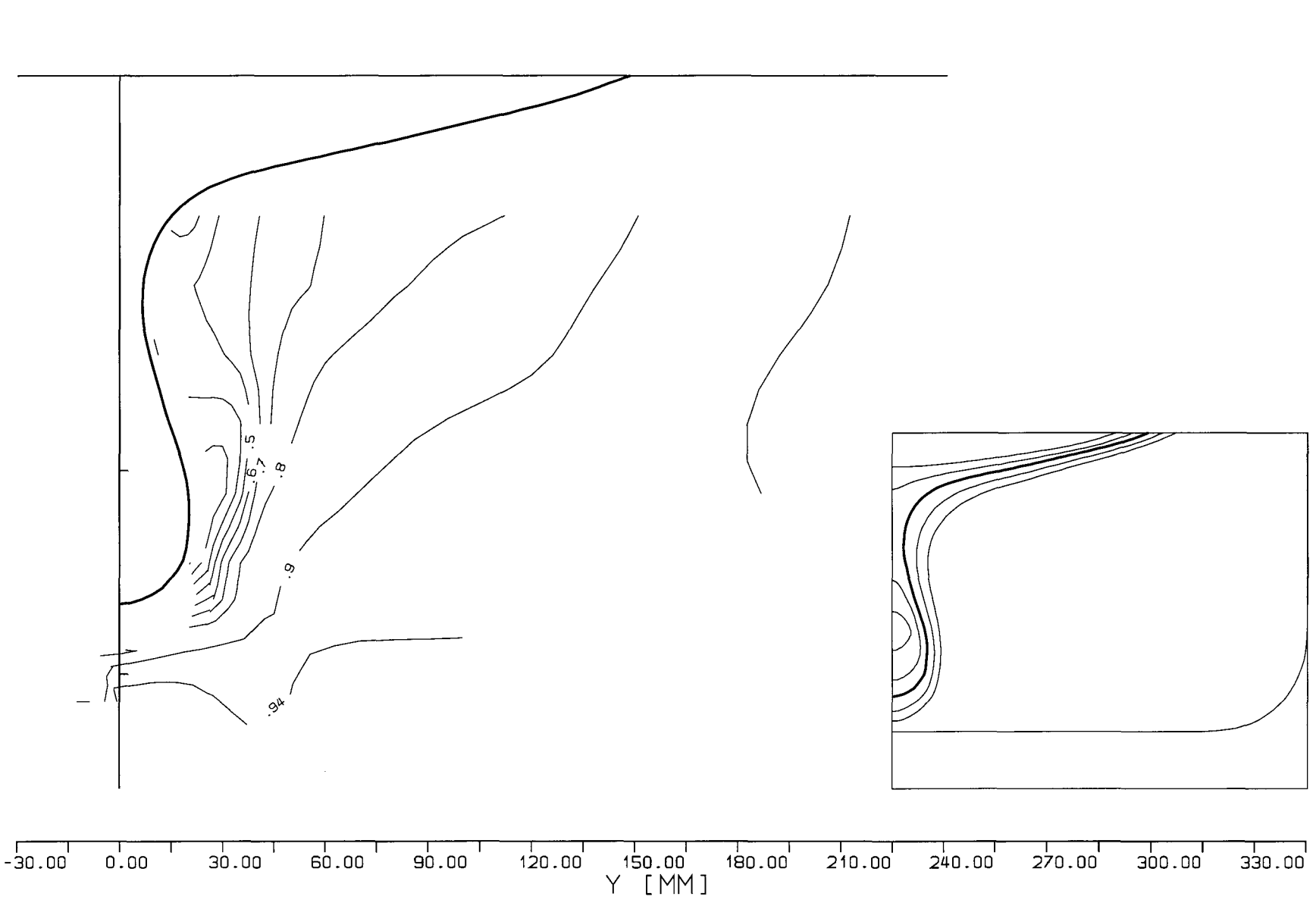

Fig. 17 Isolines of axial velocity u
X = -8.0 mm (0.95253)

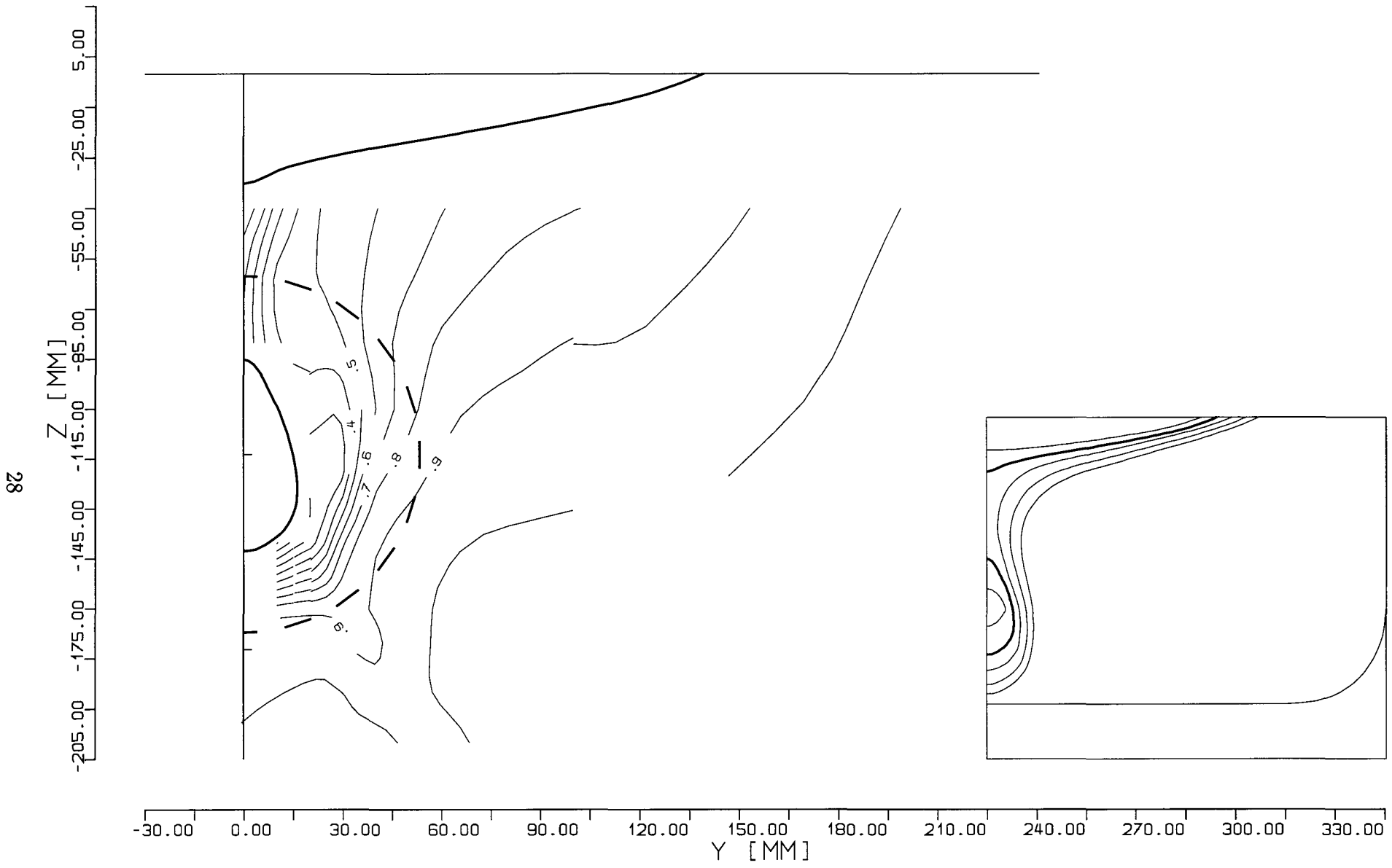

Fig. 18 Isolines of axial velocity u
X = 9.0 mm (0.95884)

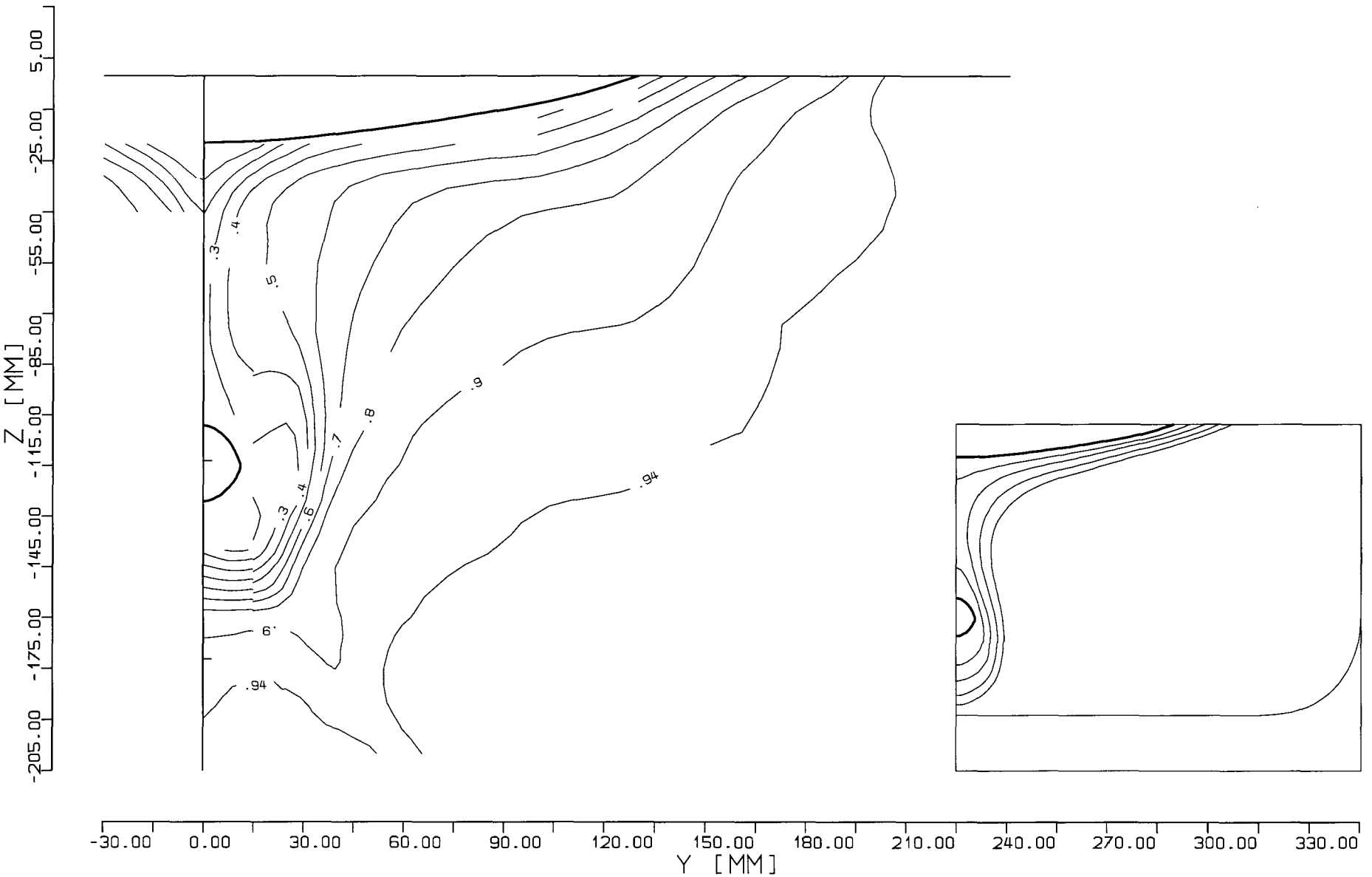

Fig. 19 Isolines of axial velocity u
X = 30.0 mm (0.96662)

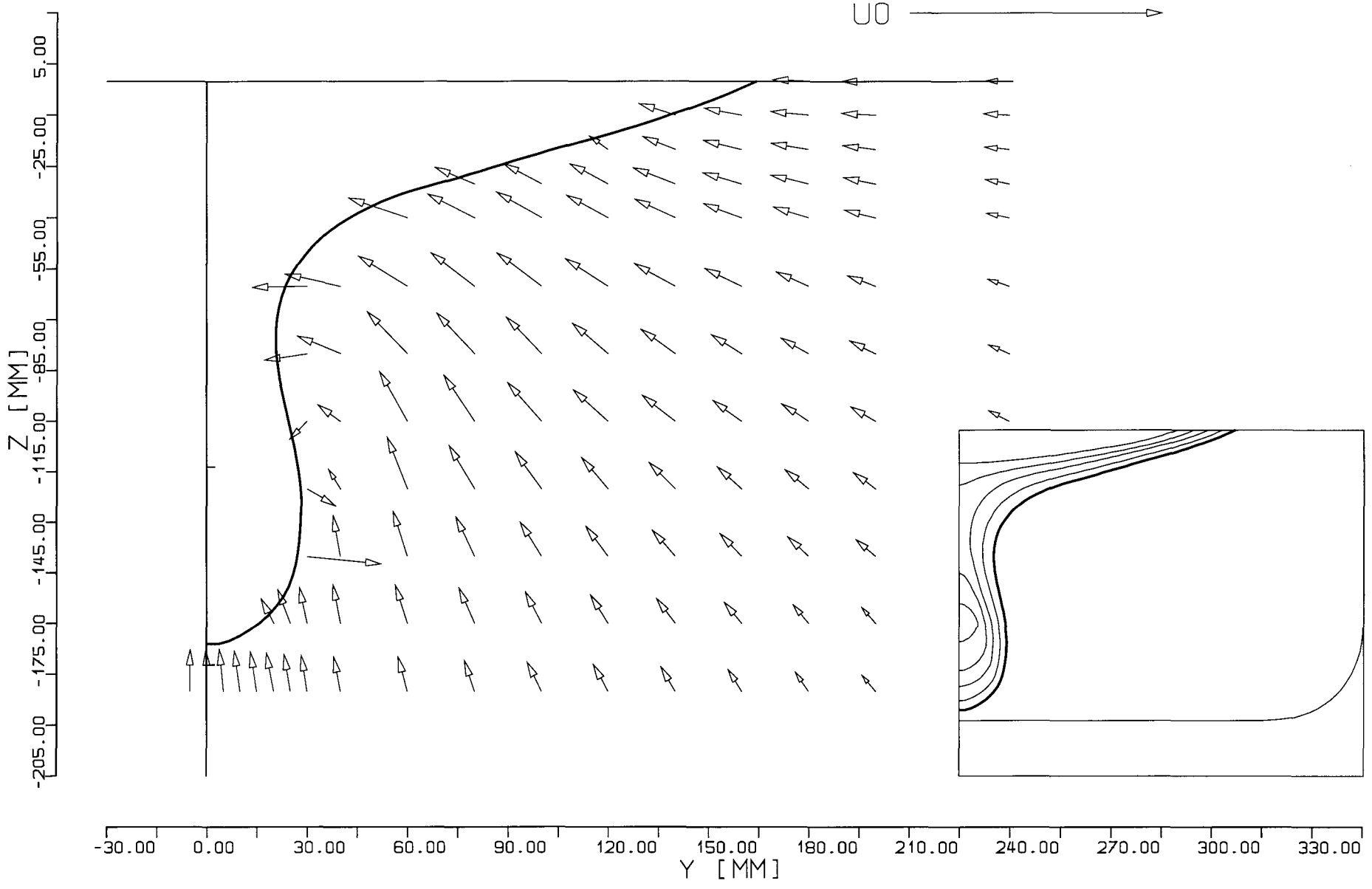

Fig. 20 Arrows of transverse components
X = -50.0 mm (0.93696)

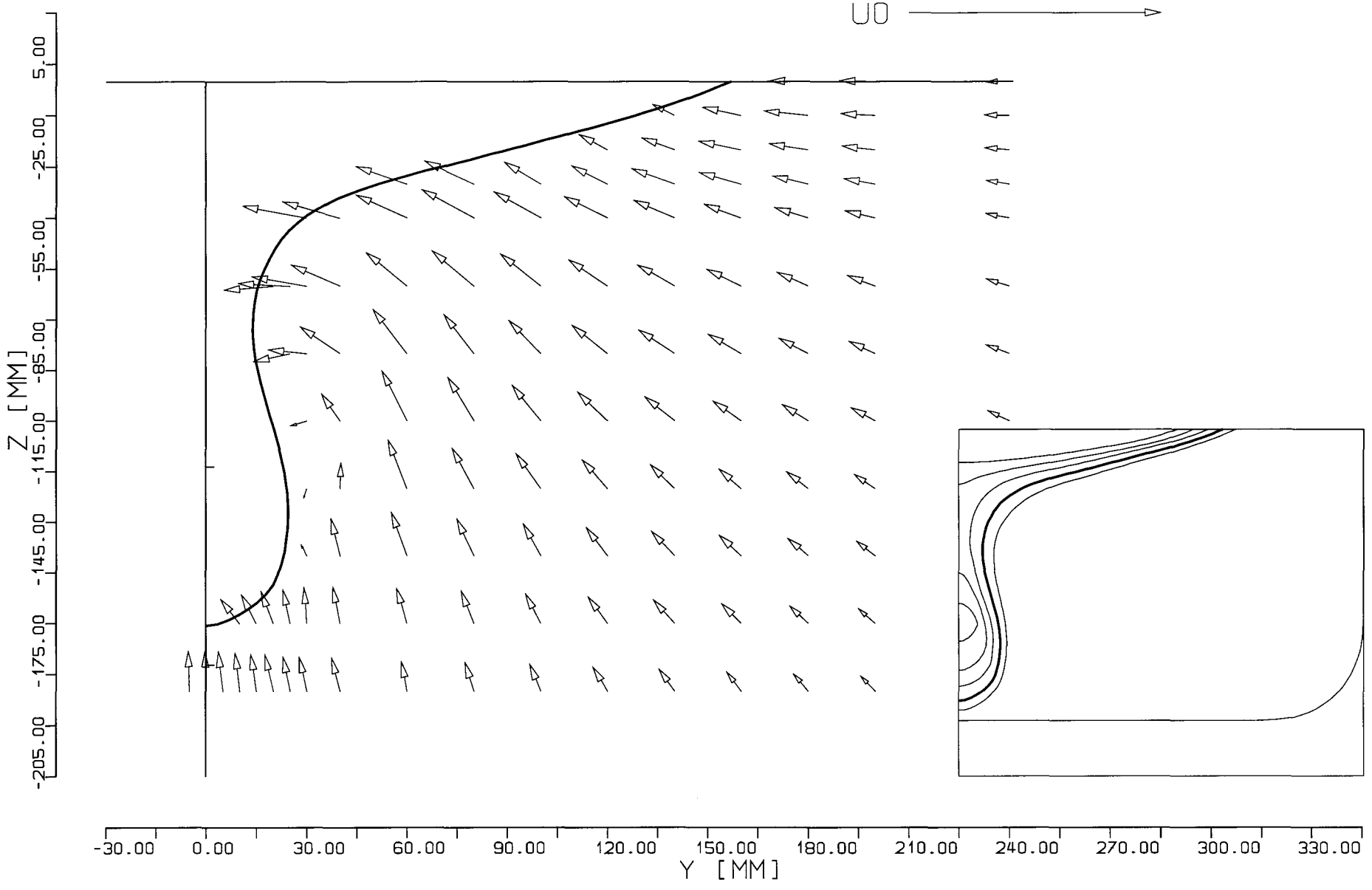

Fig. 21 Arrows of transverse components
X = -29.0 mm (0.94474)

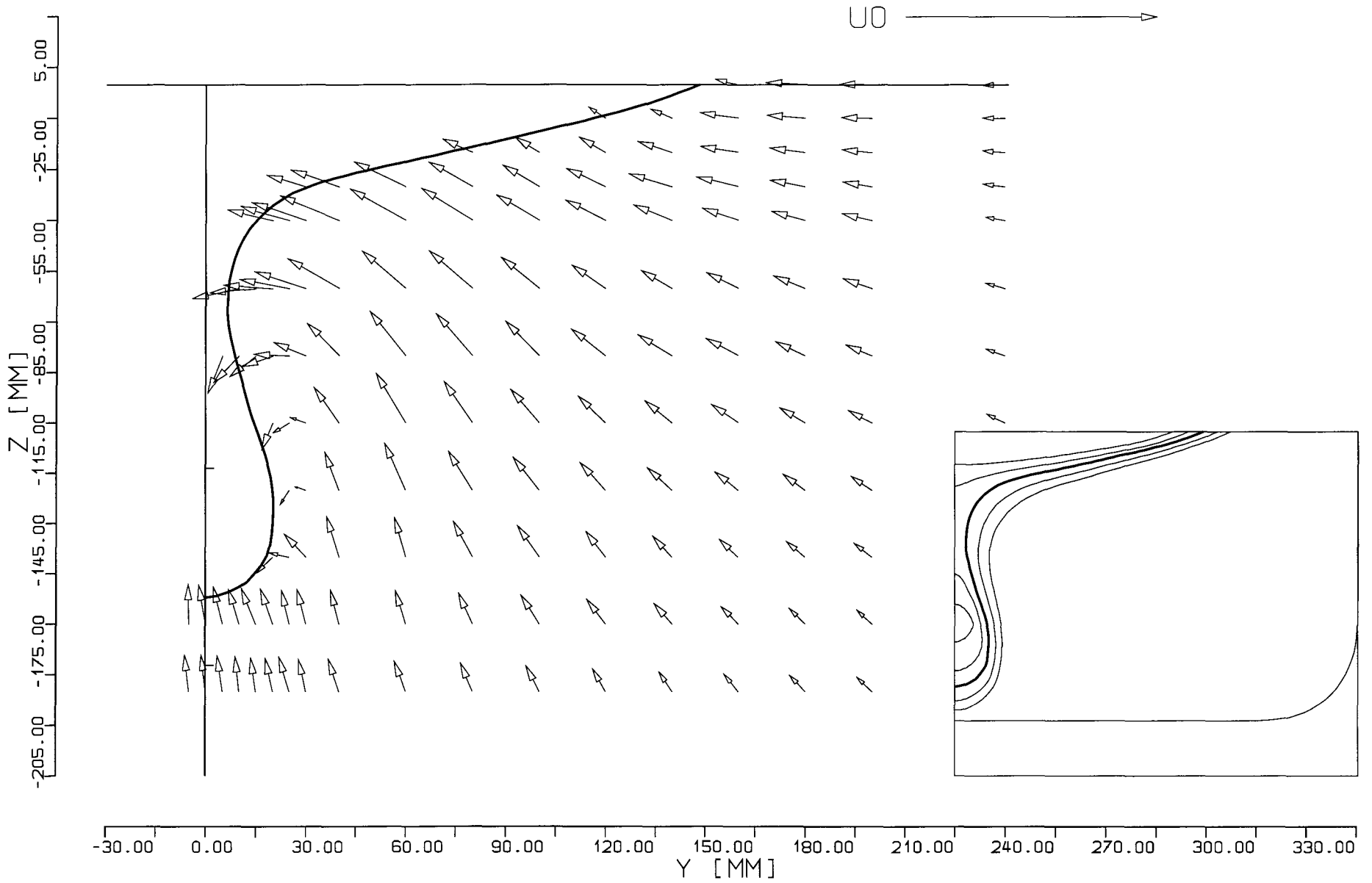

Fig. 22 Arrows of transverse components
X = -8.0 mm (0.95253)

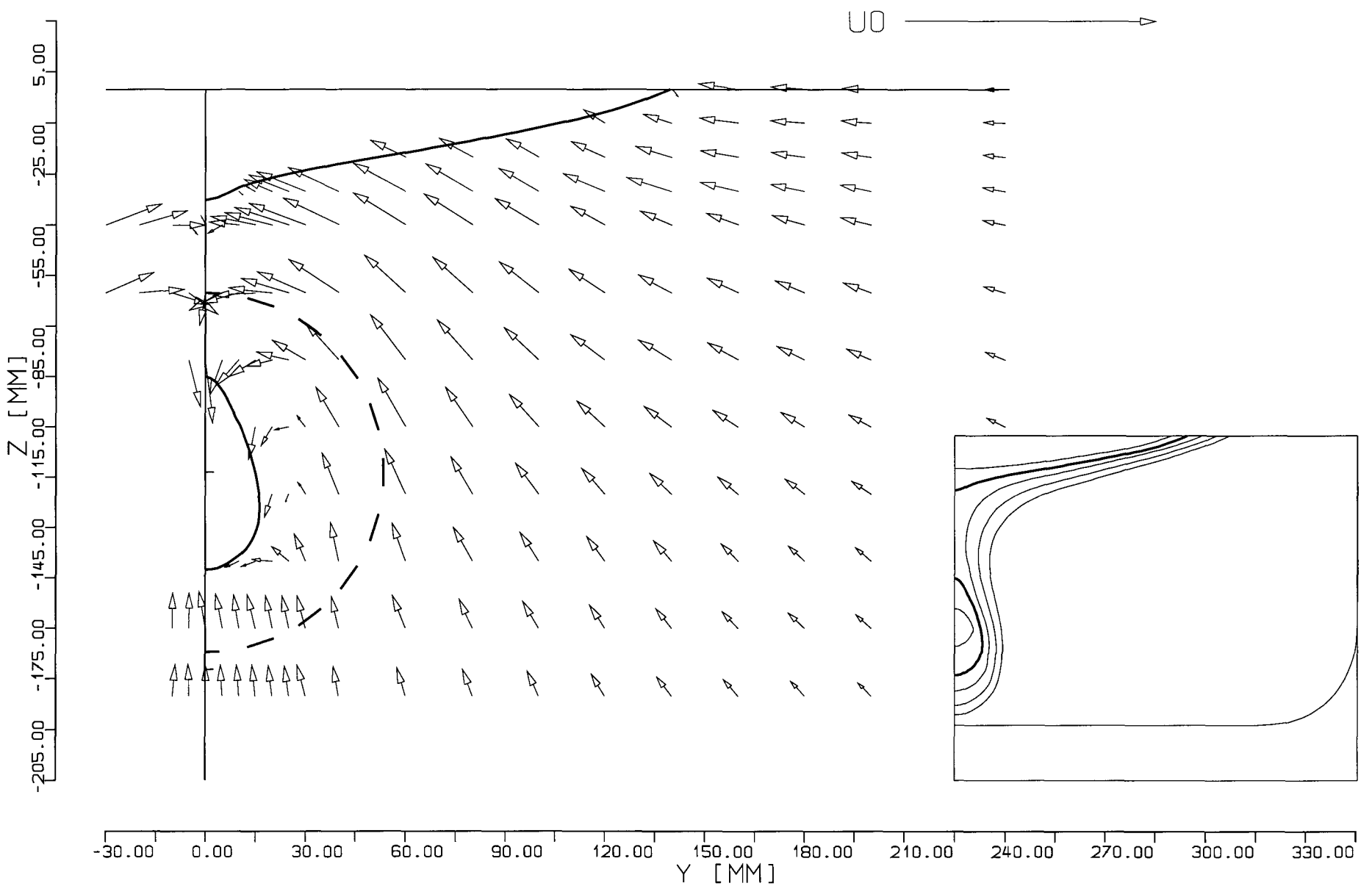

Fig. 23 Arrows of transverse components
X = 9.0 mm (0.95884)

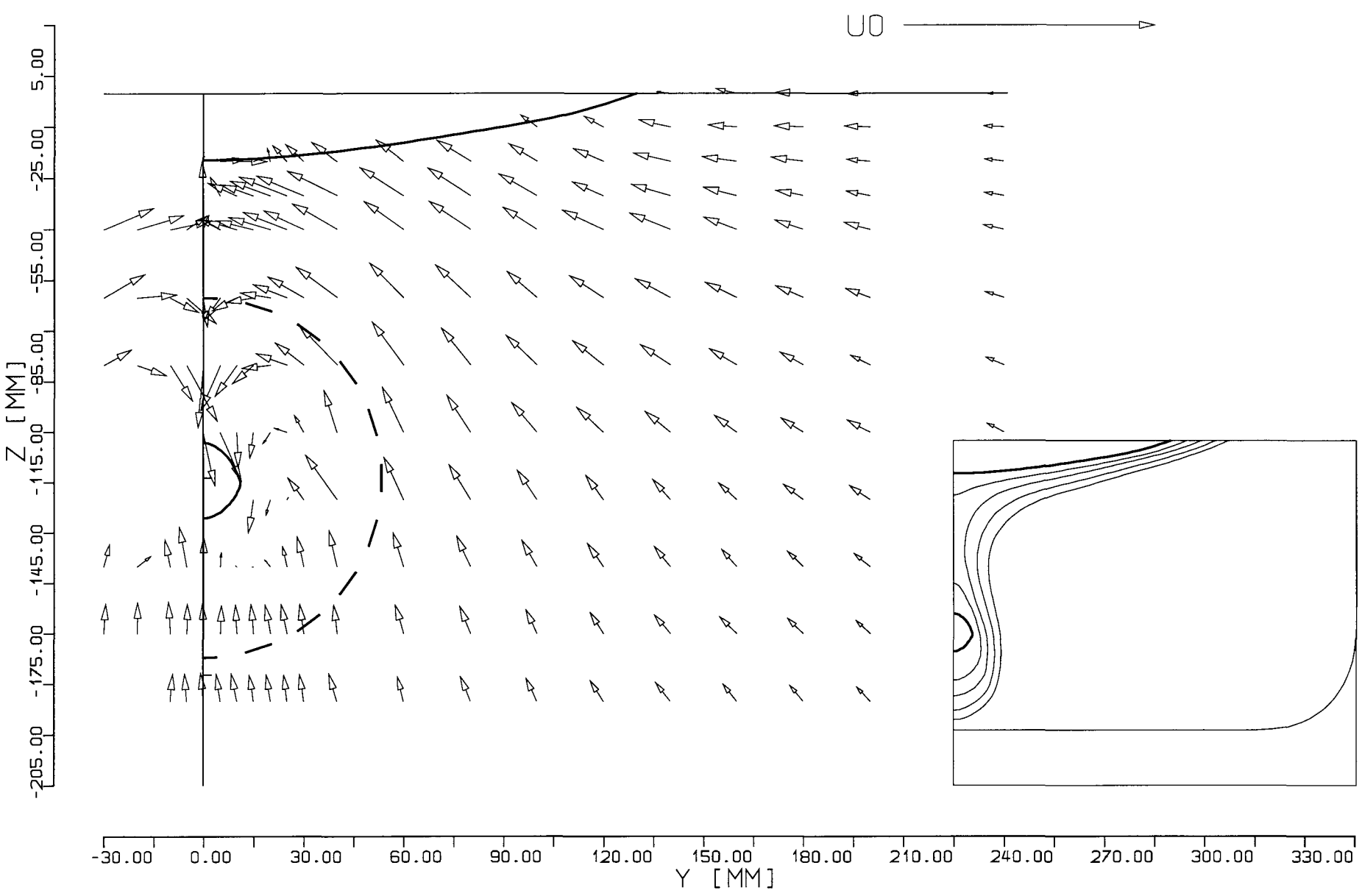

Fig. 24 Arrows of transverse components
X = 30.0 mm (0.96662)

iii) Far Wake

This plane was chosen to evaluate the final stage of the far wake of the model. A location farther downstream would be preferable (because of a better approach to the zero gradient condition relative to X), but was not possible due to the restriction given by the length of the measuring section.

The structure of the isolines (fig. 26) is determined by the wake of the (blunt towards the waterline) ending stern and the propeller boss. In both areas u falls short of 0.84 . Between these minima the axial velocity increases up to u = 0.92 . The isolines of this area show us a characteristic decrease of the diameter of the decelerated flow region. It can be explained by the effect of the transverse components. They produce a transport of undisturbed flow into the decelerated wake. Therefore the velocity in the outer part of the wake increases while the decelerated flow in the core of the wake is displaced downward.

The ascent to the velocity level of the undisturbed flow near to the model (isoline u = 0.995) takes place with a maximum of axial velocity gradient of du/dy = 0.001/mm. The non-regular extent of the isoline u = 0.995 indicates an area with neglilible gradient in axial velocity (i.e. up to u = 1.000)

A striking phenomenon is the imperfect symmetry of the flow. Experiments of A. Tasdemir showed that this is caused by a minimal disturbance in the setting chamber of the wind tunnel.

Because the model forces a symmetric border condition on its surface in all four quadrants, this effect becomes neglible near to the model.
But in locations farther downstream the influence of the models symmetry decreases, the effect of the symmetric induced transverse components decreases too. For that reason the disturbance becomes visible.

A rough estimate of the value of the disturbance velocity is obtained from the following calculation:
The plane of symmetry of the core of the wake appears to be rotated by 15^o in the clockwise direction. With a radius of rotation of 20 mm (half the distance between left and right minimum) the circumferential velocity therefore becomes 0.006 (i.e. 0.6% of U_∞).

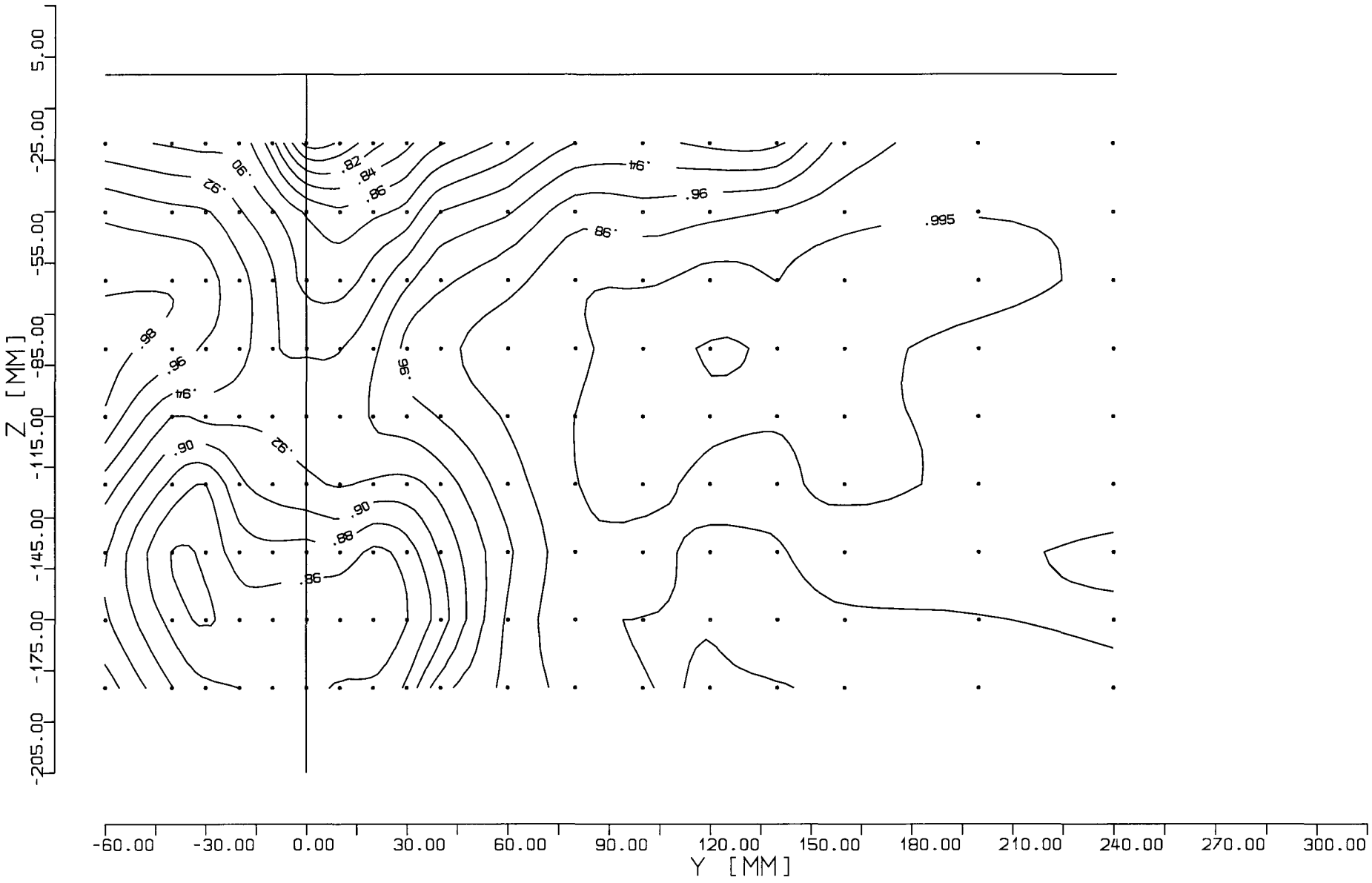

Fig. 25 Isolines of axial velocity u
X = 900.0 mm (1.28926)

5.4.2 Turbulence

The quality of the LDV-measurements allow the calculation of elements of the Reynolds-Stress-Tensor. In the following u'^2 will be treated. To make clear the relation to the often used degree of turbulence Tu it should be noted that $u'^2 = 0.01$ corresponds to Tu = 10%. The turbulence of the undisturbed flow of the wind tunnel corresponds to a quantity Tu of less than 1%. Other elements of the Reynolds-Stress-Tensor and the often used turbulent energy "k" are not presented because of the type of measurements. Nevertheless some statements about "k" are possible. From the evaluation of the measured data (i.e. using the oblique coordinate system of the LDV device) it can be stated that the fraction of turbulent energy of each transverse component is of the same order as u'^2, but smaller in the most cases. Thus u'^2 may be used as an estimate for k. The distribution of u'^2 is shown at the following stations:

i) Main Frame

The isolines of $u'^2 = 0.01$ (fig. 27) follow the course of the isolines for the u-component. Proceeding from the waterline to the bilge we observe the isolines parallel to the surface. A reduction of wall distance takes place half around the bilge, followed by a monotonic increase of wall distance towards the keel.

The incompleteness of the isolines at the bilge is due to certain difficulties. There exist some points near the bilge where a nearly direct reflection of the laser beams into the receiving optic takes place. Thus at these points a lot of additional noise appears in the LDV-output leading to a virtual increased level of turbulence.

ii) Propeller Boss

Similar to u, the "outer area" of the flow is marked by a diagonal isoline of $u'^2 = 0.002$ in all five planes (fig. 28 to 32). The beginning of the bilge vortex is indicated by the structure of the turbulence intensity pattern. In the area with a maximum of shear flow the turbulence reaches its maximum too. Around it we find a reduced intensity of turbulence. The planes farther downstream additionally show the turbulence produced by the boundary layer near to the waterline. For example the last plane shows us an extended horizontally oriented area of increased turbulence, which reaches 20 mm away from the surface (isoline $u'^2 = 0.004$).

iii) Far Wake

The structure of the isolines of u'^2 (fig. 33) is mainly equivalent to the structure of the isolines for the u-component. The isoline $u'^2 = 0.002$ and the "outer area"-isoline u = 0.98 coincide in the whole plane. Similar to the bilge vortex at the propeller boss, the maximum of turbulence intensity is located in the region of strong shear. A main difference should be mentioned, the gradient du/dy at this downstream station is reduced by an order of magnitude relative to the gradient at the propeller boss.

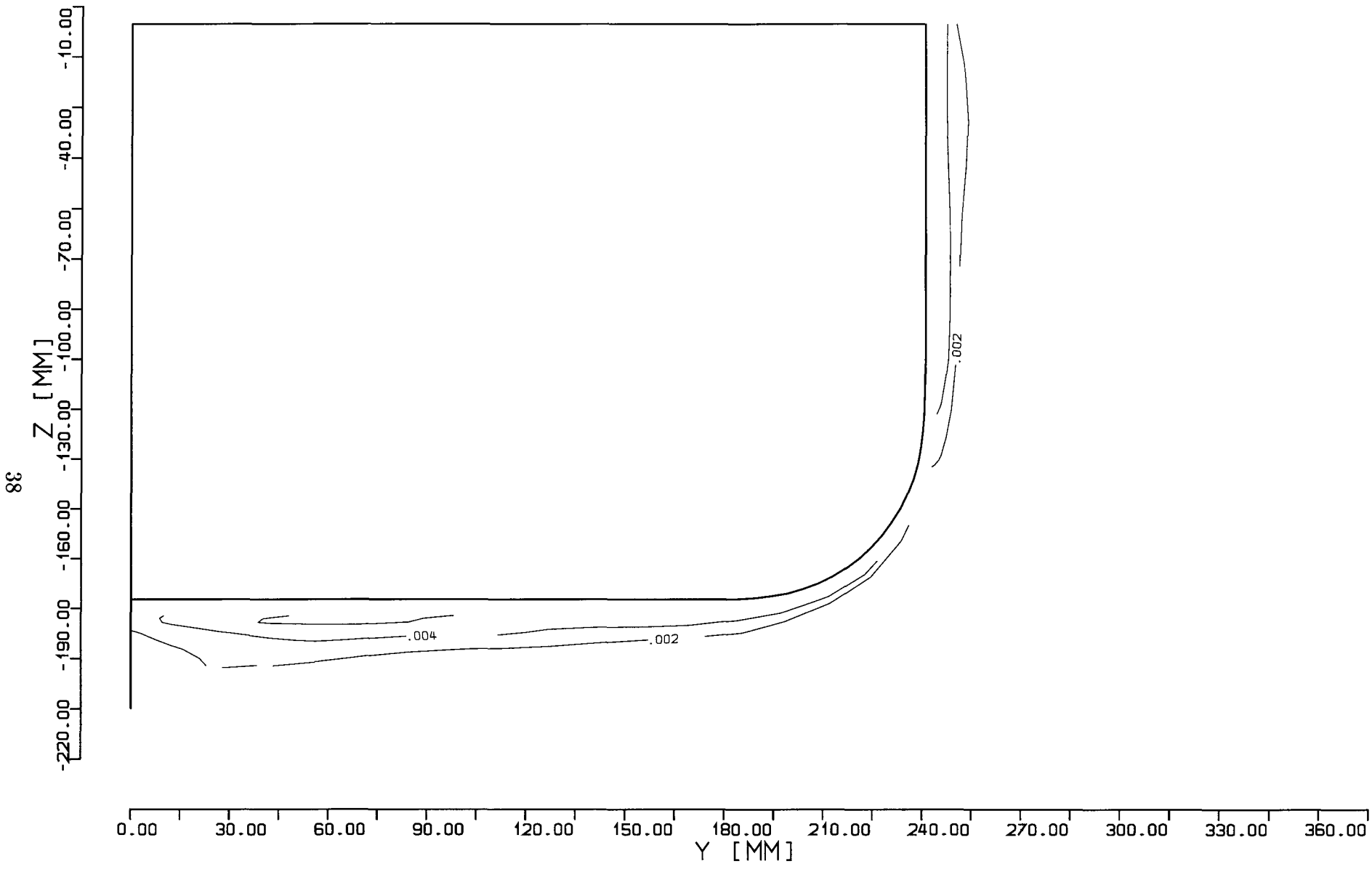

Fig. 26 Isolines of u'^2
X = -1093.0 mm (0.55016)

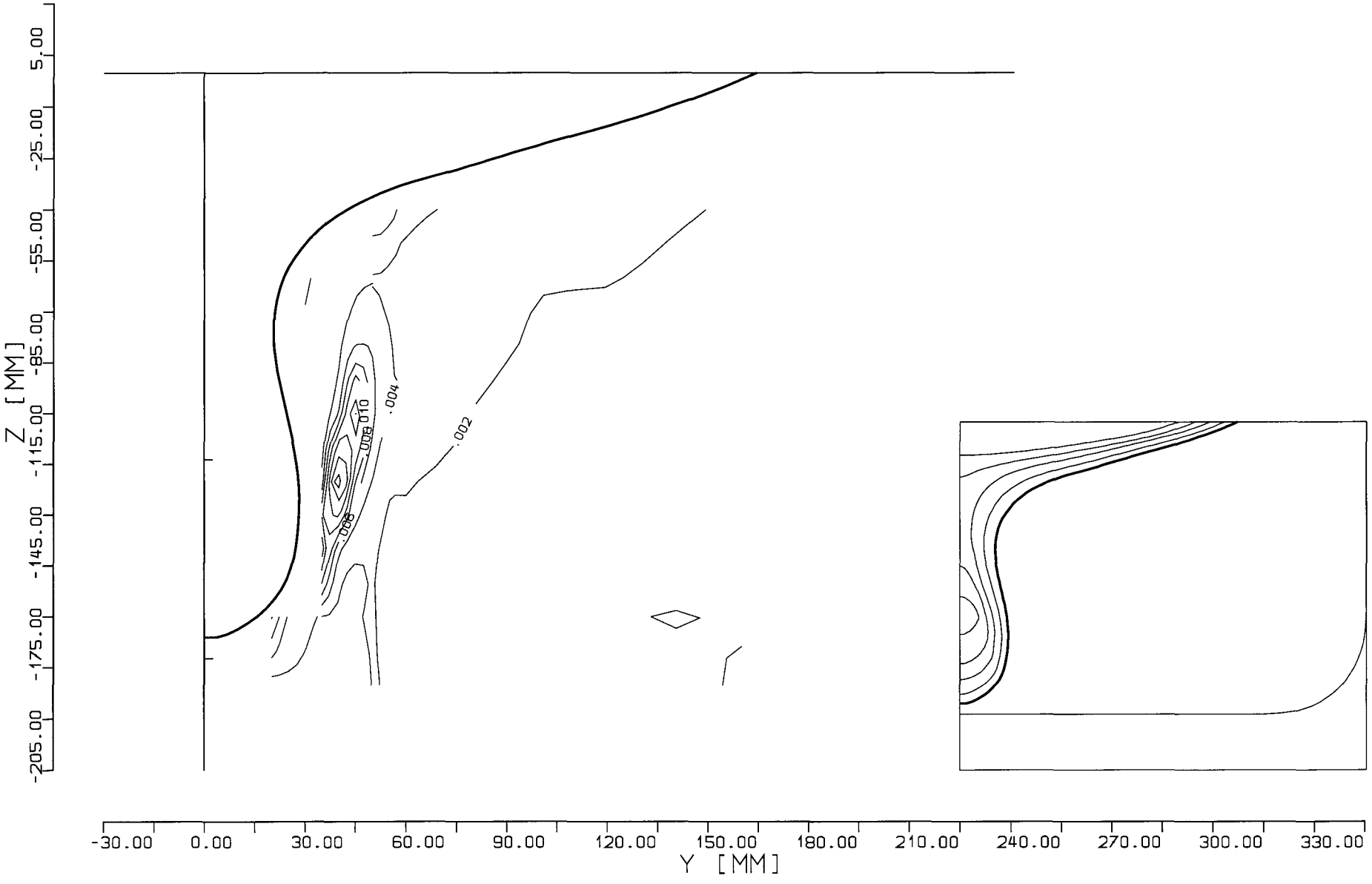

Fig. 27 Isolines of u'^2
X = -50.0 mm (0.93696)

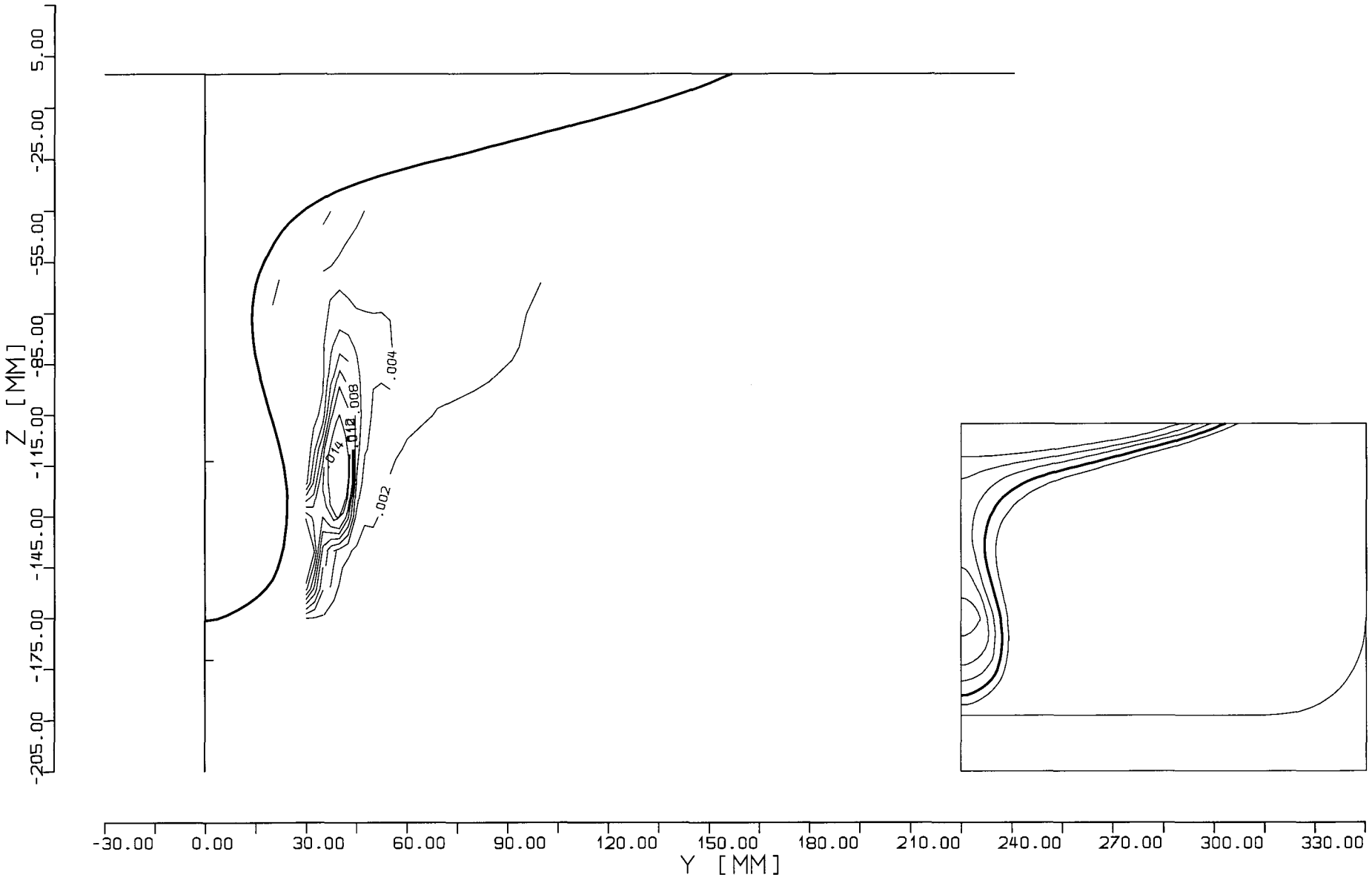

Fig. 28 Isolines of u'^2
X = -29.0 mm (0.94474)

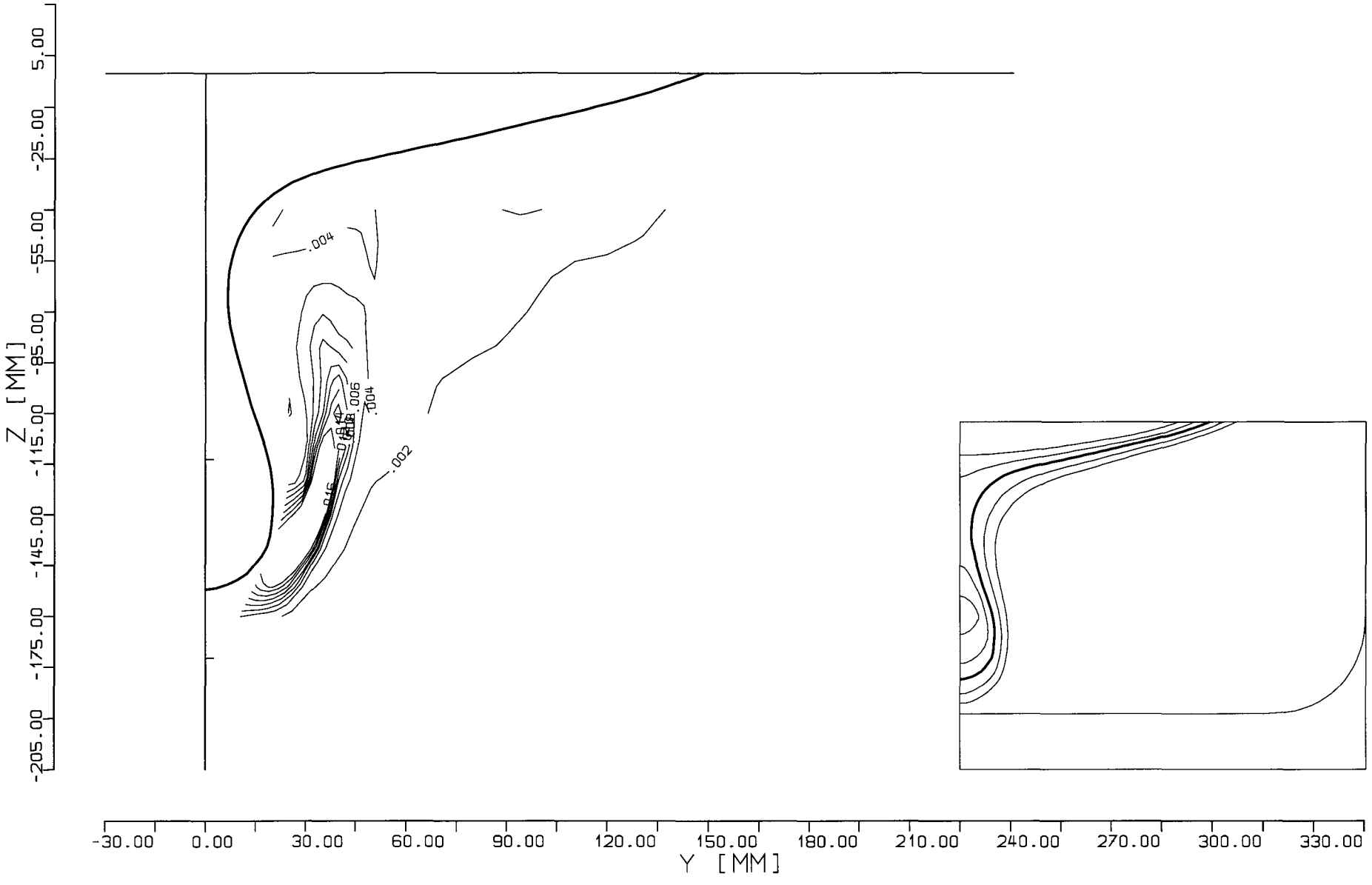

Fig. 29 Isolines of u'^2
X = -8.0 mm (0.95253)

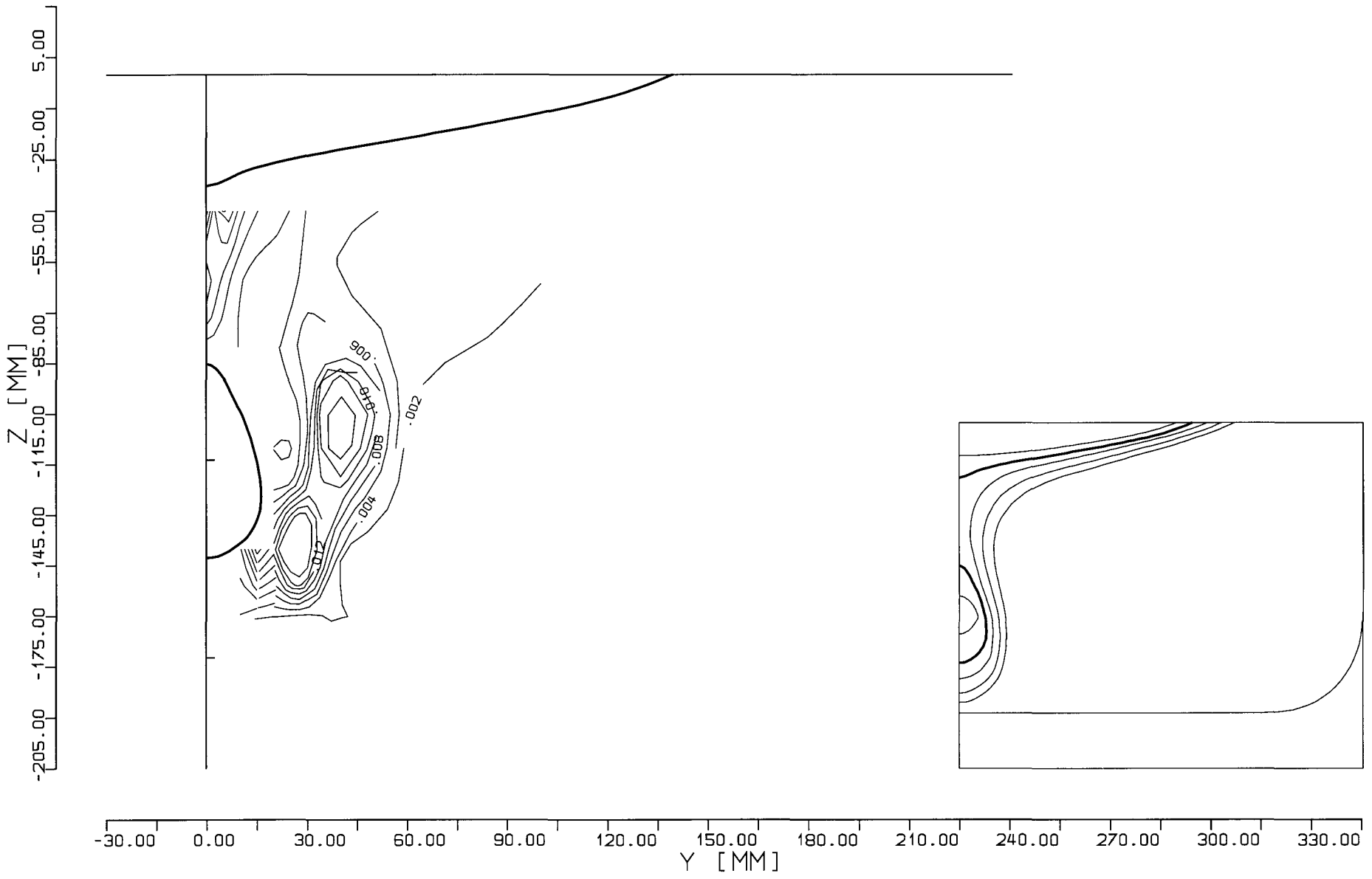

Fig. 30 Isolines of u'^2
X = 9.0 mm (0.95884)

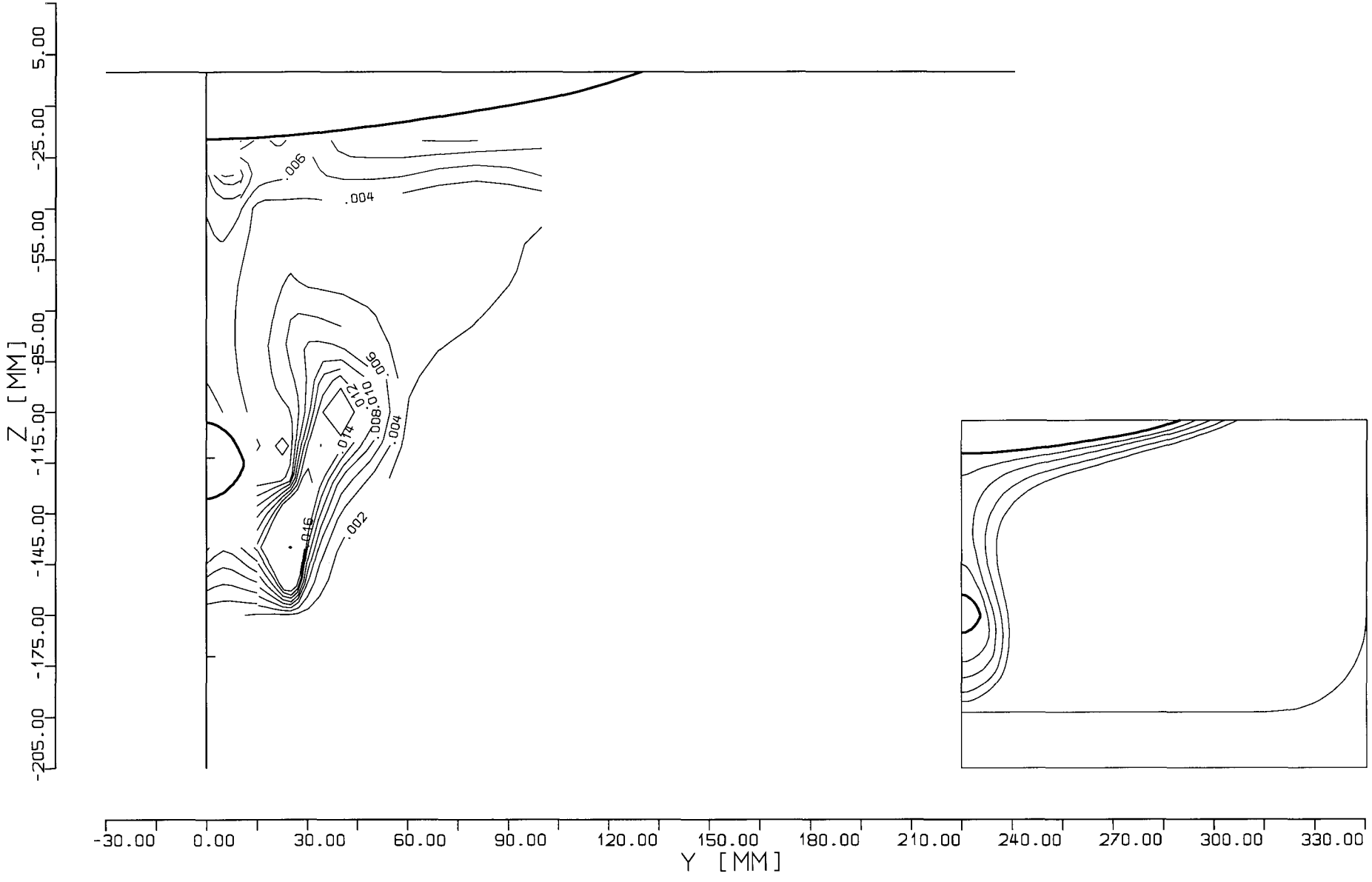

Fig. 31 Isolines of u'^2
X = 30.0 mm (0.96662)

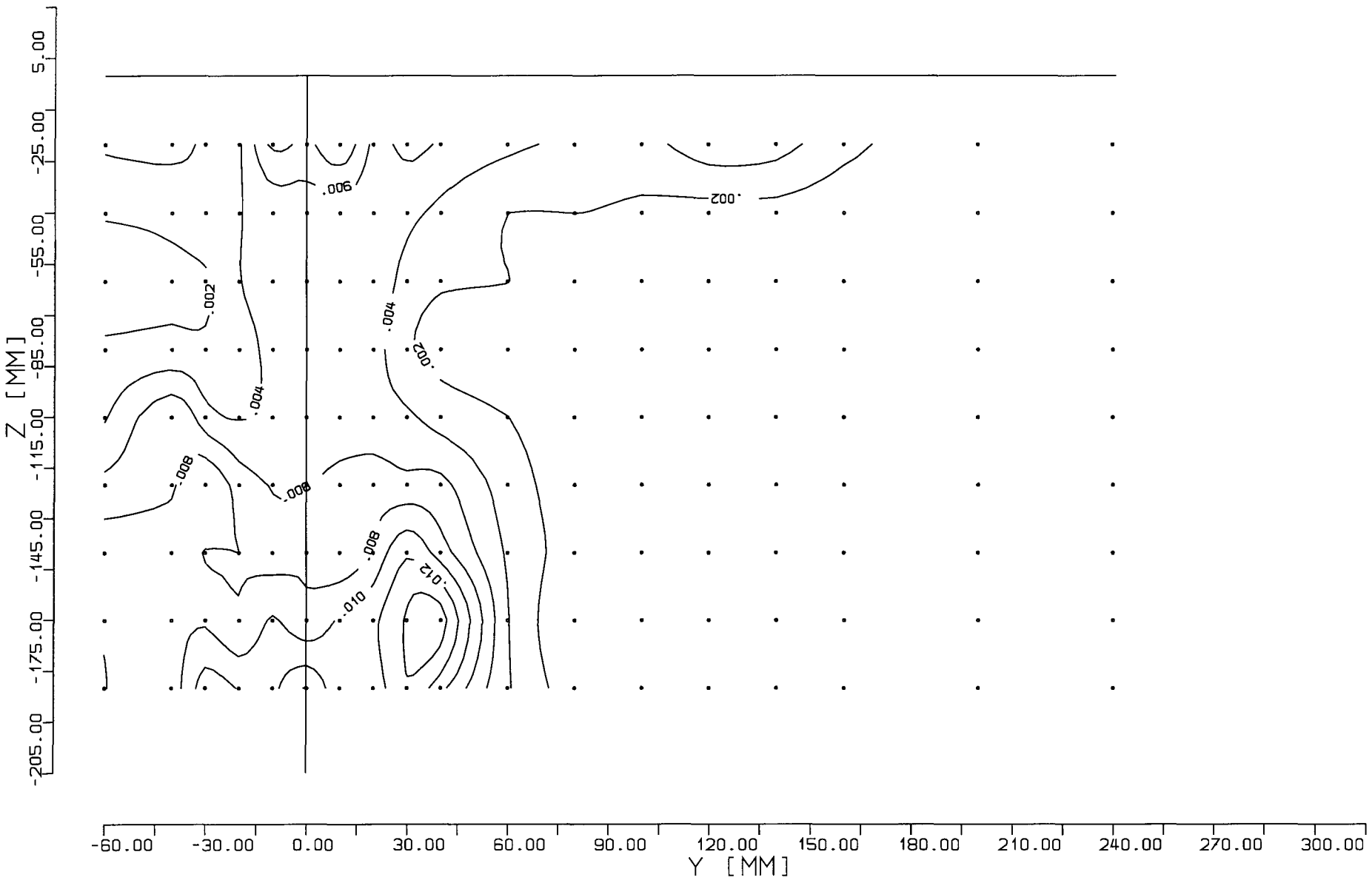

Fig. 32 Isolines of u'^2
X = 900.0 mm (1.28926)

Nomenclature

Lpp	length between perpendiculars
U_∞	incident velocity, 27 m/sec
X,Y,Z	coordinate system, units in mm (Default) or nondimensionalized by Lpp (ref. Appendix) X parallel to U_∞ Y normal to the X-Z-plane Z from the keel to the waterline
X_{LDV}, Y_{LDV}, Z_{LDV}	coordinates in units of mm, origin at the stern (ref. Appendix)
X_{Lpp}, Y_{Lpp}, Z_{Lpp}	coordinates in units of Lpp, origin at the bow (ref. Appendix)

Cp	pressure coefficient
U V W	dimensional mean velocity components
u v w	dimensionless mean velocity components, normalized by U_∞
u'^2	first component of the Reynolds Stress Tensor
k	turbulent kinetic energy

Acknowledgements

The authors wish to thank the federal ministry "Bundesministerium für Forschung und Technologie" for funding the research project "Hamburg Test Case" at the IfS.

The HSVA was very helpful with the original body plan and the data of the container ship and cooperated to determine similarly located measuring planes.

Thanks a lot to Mr. Schuckert and Mr. Meister from the IfS for their help during our activities in the wind tunnel.

Last but not least we wish to thank all the members of the IfS who contributed with innumerable pieces of work to the project.

References

[1] Bertram V., Chao K.Y., Lammers G., Laudan J.: Entwicklung und Verifikation Numerischer Verfahren zur Antriebsleistungsprognose, Phase 2, HSVA-Report Nr. 1579, 1992

[2] Bradshaw P., Cebeci T.: Momentum Transfer in Boundary Layers, Hemisphere Publishing Corporation; Washington, London 1977, 1. Auflage

[3] Cummins H.Z., Yeh Y.: Localized Fluid Flow Measurements with a He-Ne-Laser-Spectrometer, Applied Physics Letter, Vol. 4, No. 10, 1964

[4] Denker J., Knaack T., Kux J.: Experimental and Numerical Investigations of HSVA-Tanker-2 Flow Field, IfS-Report Nr. 521, Hamburg May 1992

[5] Driver D.M., Johnston J.P.: Three-Dimensional Boundary Layer Flow with Streamwise Adverse Pressure Gradient, 10. Australasian Fluid Mechanics Conference, University of Melbourne 11.-15. Dezember 1989

[6] Durrani T.S., Greated C.A.: Laser Systems in Flow Measurement, Plenum Press, New York 1977

[7] Durst F., Melling A., Whitelaw J.H.: Principles and Practice of Laser-Doppler Anemometry, Academic Press, London 1981, 2. Auflage

[8] Fry D.J., Huang T.T., Jessup S.: Application of Laser Doppler Velocimetry for Ship Hydrodynamic Measurements, ITTC-Report, October 1987

[9] Graham J.A.H., Phillips W.R.C.: Reynolds-stress measurements in a turbulent trailing vortex, Journal of Fluid Mechanics 1984, Volume 147

[10] Hochbaum A.,Sames P., Kux J.: Proceedings of CFD Workshop Volume I, Ship Research Institute, Tokyo March 1994

[11] Hoffmann H.P.: Untersuchung der dreidimensionalen, turbulenten Grenzschicht an einem Schiffsdoppelmodell im Windkanal, IfS-Report Nr. 343, Hamburg 1976

[12] Knaack T.: Untersuchung der Struktur des Reynolds Tensorfeldes in einer dreidimensionalen Strömung, Dissertation/IfS-Report Nr.527, Hamburg November 1992

[13] Knaack T., Kux J., Wieghardt K.: On the Structure of the Flow Field on Ship Hulls, Osaka International Colloquium on Ship Viscous Flow, Osaka 1985, Proceedings, Tanaka, Suzuki, Himeno, Herausgeber: Osaka University and University of Osaka Prefecture

[14] Kux J., Wieghardt K.: Nomineller Nachstrom auf Grund von Windkanaluntersuchungen, Jahrbuch Schiffbautechnische Gesellschaft 74, 1980

[15] Lammers G., Laudan J., Stöhrmann H.: Applicability of Laser Doppler Velocimetrie to Marine Engineering Research, ITTC-Report, October 1987

[16] Lammers G., Laudan J., Stöhrmann H.: Korrelation von Nachstrom, Kavitation und deren Folgeerscheinungen, Teil A: Nachstrom, HSVA-Report Nr. 1565, March 1989

[17] Larsson L., Patel V.C., Dyne G.: Ship Viscous Flow: Proceedings of the 1990 SSPA-CTH-IIHR Workshop

[18] Laufer J.: The Structure of Turbulence in Fully Developed Pipe Flow, NACA Report 1174, 1954

[19] Wieghardt K.: Der Windkanal des Instituts für Schiffbau, Schrift Nr. 2247, December 1975

[20] Wieghardt K.: Zur Struktur turbulenter Strömungen, IfS-Report Nr. 470, October 1986

[21] Patel V.C.: Ship Stern and Wake Flows: Status of Experiment and Theory, 17. ONR Symposium on Naval Hydrodynamics, The Hague, The Netherlands, 29.8-2.9.1988

[22] Scheinpflug M.: Vergleichende Nachstromuntersuchungen an einem Schiffsdoppelmodell im Windkanal mit einem Laser-Doppler-Anemometer und Drucksonden, IfS-Report Nr. 381, October 1979

[23] Strunck V.: Untersuchung grossräumiger Strukturen im Nachlauf einer längsangeströmten ebenen Platte, DFVLR-Report/Dissertation Göttingen, July 1987

[24] Orloff K.L.: Trailing Vortex Wind-Tunnel Diagnostics with a Laser Velocimeter, Journal of Fluid Mechanics, Volume 11, No. 8, August 1974

List of Figures

Appendix

The contour of two parts of the wind tunnel model, the stern (left side) and the bulbous bow (right side), is shown in the equally scaled fig. 34 (scale 1:2 relative to the model). Because of the trim of 0.41^{o} the draught decreases from the stern to the bow, leading to a gap in the line of the keel between the two parts. This gap is closed by the long middle part of the ship (not drawn).

Two equally scaled axes for both the stern (lower axis) and the bow (upper axis) give the streamwise position in units of two coordinate systems:

The so called "LDV-coordinates" are represented by the downward tics. They give the coordinates in units of *mm* in the model scale. The origin (symbol "o" in fig. 34) and the orientation of the X-, Y- and Z-axis is explained by the three arrows at the stern. The definition of the origin reflects its function to support the LDV-measurements by characteristic points of the model to achieve definite and quick to find reference positions (e.g. X = 0, the dotted line in fig. 34, is placed at the foremost point in the curve of the contour of the stern).

The so called "Lpp-coordinates" are represented by the upward tics. The spacing of the tics (here 2%) is given in units of Lpp. The orientation and the origin of the coordinate system is as above. Solely the X-coordinate of the origin (symbol "x" in fig. 34) is shifted upstream to the station of the forward perpendicular. As a further reference the aft and the forward perpendiculars are marked by a straight vertical line.

Additionally the extent and the station of the LDV-measured planes at the stern are shown (dashed lines) and the plane and the diameter of the propeller is drawn (pointed line downstream of the stern, D = 6.1 m, 3.96 m upstream of the aft perpendicular for the full scale case).

Three strange features should be explained:

The upper part of the stern does not reach the aft perpendicular. This is caused by the reduced draught of the full-scale measurement conditions relative to the construction draught. Due to the reduced draught the intersection point of the "waterline" and the contour of the model is shifted upstream. Additionally the trim leaded to a very small angle between the "waterline" of the model and the contour of the stern. Because the wind tunnel model represents only the under water part of the hull, we would have a thin plate like hull (thickness only a few millimeter) at the aftmost part of the model. Because such thin parts of the model are hard to manufacture and are most likely to break, the contour of this aftmost part is changed. A piece of a circle substitutes this part of the contour, when the thickness is lower than 10 mm.

In opposite to above the forward perpendicular seems to be located at an unusual position inside the model. The impression is caused by the reduced draught which shifts the intersection point between the contour of the bulbous bow and the "waterline" to an upstream position.

As a third the main frame should be mentioned. The data as we received them from the HSVA determine the station of the main spawn at a slightly different position as most likely expected. The station is defined at X_{LDV} = -1093.4 mm (0.55001).

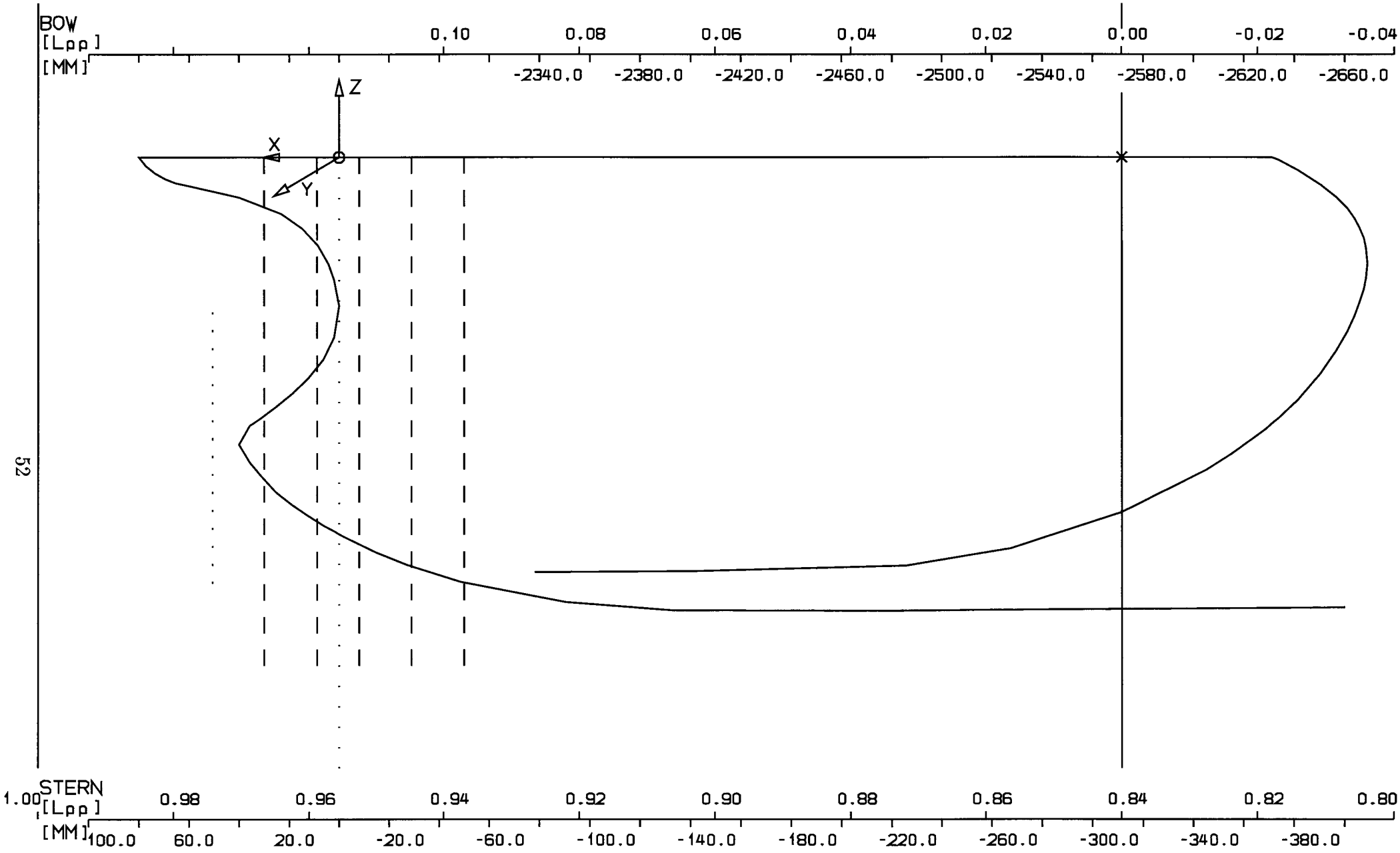

Fig. 33 Stern and Bow of the Wind Tunnel Model